Journal of Medicinal Chemistry

Article

pubs.acs.org/jmc

Identification of a Crucial Amino Acid in the Helix Position 6.51 of Human Tachykinin Neurokinin 1 and 3 Receptors Contributing to the Insurmountable Mode of Antagonism by Dual NK_1/NK_3 Antagonists

Caterina Bissantz,[†] Claudia Bohnert,[‡] Torsten Hoffmann,[†] Anne Marcuz,[‡] Patrick Schnider,[†] and Pari Malherbe*[,‡]

[†]Medicinal Chemistry and [‡]DTA CNS, pRED, Pharma Research and Early Development, F. Hoffmann-La Roche AG, Grenzacherstrasse 124, CH4070, Basel, Switzerland

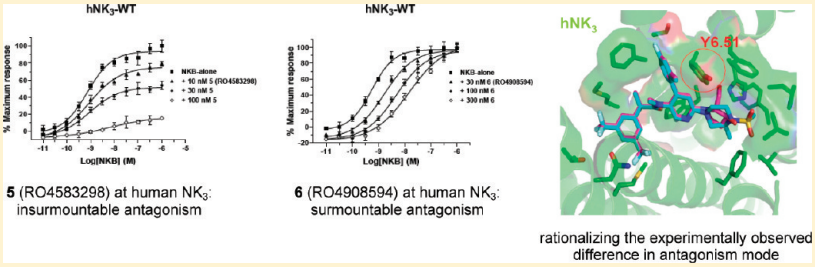

ABSTRACT: The neurokinins are neuropeptides that elicit their effect through three GPCRs called NK_1, NK_2, and NK_3. Compounds **5** and **6** are dual hNK_1 (K_i of 0.7 and 0.3 nM) and hNK_3 (K_i of 2.9 and 1.7 nM) antagonists. Both compounds exhibit an insurmountable mode of antagonism at hNK_1, whereas at hNK_3, they differ in that **5** is an insurmountable but **6** a surmountable antagonist. Using homology modeling and site-directed mutagenesis, hNK_1-Phe264 and hNK_3-Tyr315 were found to be the molecular determinants of hNK_1 and hNK_3 antagonism by **5** and **6**. In [^{3}H]IP studies, the mutation hNK_1-F264Y converted the mode of action of **5** from insurmountable to partial insurmountable antagonism while it had no effect on that of **6**. Conversely, the mutation hNK_3-Y315F enhanced the insurmountable behavior of **5** and converted **6**'s surmountable to an insurmountable antagonism. This finding was further confirmed by characterizing additional derivatives of **5** and **6**, most notably with a hybrid structure.

INTRODUCTION

Schizophrenia is a debilitating mental disorder that affects 0.5−1% of the general population. It is characterized by positive (delusions, hallucinations, and paranoia), negative (apathy and lack of social interaction), and mood (anxiety, dysphoria and suicidality) symptoms, as well as cognitive impairment (memory and attention deficits).[1] Current therapies, mainly based on antagonizing D_2/5-HT_{2A} receptors, are largely effective against positive symptoms but have a limited efficacy in the treatment of negative and cognitive symptoms. These treatments also suffer from several side effects including weight gain, diabetes, and extrapyramidal symptoms.[2] The results of randomized double-blind placebo controlled phase II clinical trials of (*S*)-(+)-*N*-((3-[1-benzoyl-3-(3,4-dichlorophenyl)-piperidin-3-yl]prop-1-yl)-4-phenylpiperidin-4-yl)-*N*-methylacetamine (osanetant, SR 142801)[3,4] and (*S*)-(−)-*N*-(α-ethylbenzyl)-3-hydroxy-2-phenylquinoline-4-carboxamide (talnetant, SB 223412),[5,6] two potent non-peptide antagonists of the neurokinin 3 receptor in schizophrenia patients, have suggested a significant improvement in psychopathology including positive symptoms, with improved efficacy, but a lower propensity to induce side effects.[7−9] Thus, neurokinin 3 receptor antagonism represents an alternative therapeutic approach for the treatment of schizophrenia.[10]

The family of neurokinin (NK, also called tachykinin) peptides is composed of substance P (SP), neurokinin A (NKA), and neurokinin B (NKB), which act as neurotransmitters/neuromodulators and elicit their effects through three types of neurokinin receptors, NK_1, NK_2, and NK_3 (nomenclature follows Alexander et al.[11]). The NK receptors belong to the class A family (rhodopsin-like) of G-protein-coupled receptors (GPCRs) that are coupled via $G_{q/11}$ to the activation of the phospholipase C-IP3/DAG signaling pathway leading to an elevation of intracellular Ca^{2+} levels.[12,13] Among NK receptors, NK_3 receptors are of particular interest because of their possible role in the pathophysiology of schizophrenia.[7,9] Preclinical studies have demonstrated the involvement of NKB/NK_3-mediated activation in the release of dopamine, especially in the ventral and dorsal striatal regions.[14] Interestingly, acute administration of compound **4** (talnetant) produced significant increases in extracellular dopamine and noradrenalin in the medial prefrontal cortex of guinea pigs.[15] SP/NK_1 signaling plays a major role in the modulation of stress responses and in the regulation of affective behavior. It has been shown that various emotional stressors increase SP efflux

Received: December 19, 2011
Published: May 10, 2012

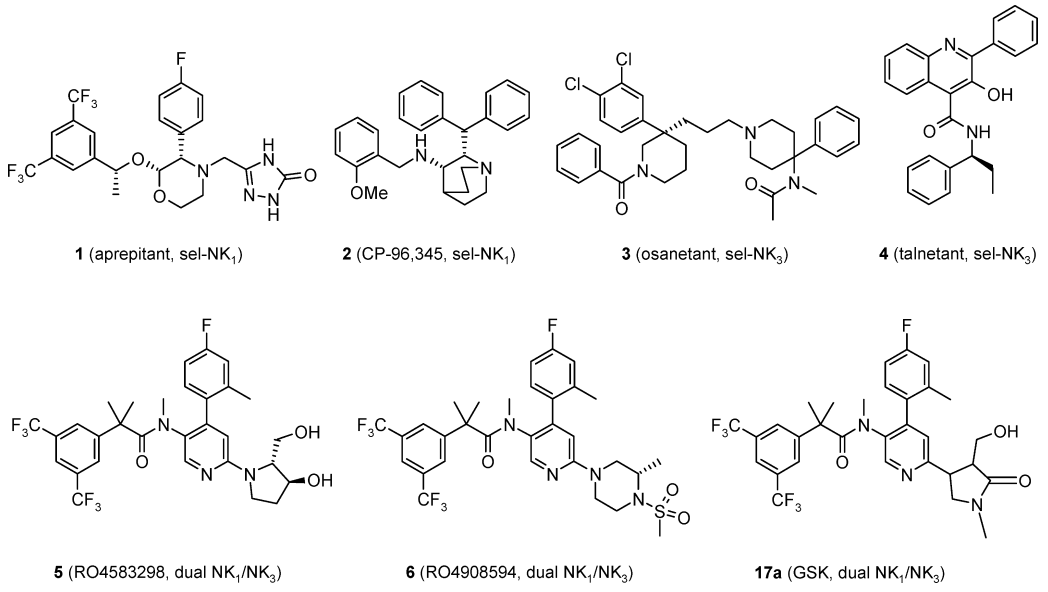

Figure 1. Chemical structures of the selective NK_1, NK_3, and dual NK_1/NK_3 antagonists.

in discrete forebrain areas such as amygdala and septum.[16] The pharmacological blockade or genetic disruption of NK_1 expression has been shown to result in a marked reduction of anxiety and stress-related responses and also increased 5-HT-mediated function.[17,18] Although the NK_1 receptor antagonists 2-(*R*)-(1-(*R*)-3,5-bis(trifluoromethyl)phenylethoxy)-3-(*S*)-(4-fluoro)phenyl-4-(3-oxo-1,2,4-triazol-5-yl)methylmorphine) (aprepitant, MK-869),[19] L-759274,[20] and (+)-(2*S*,3*S*)-3-(2-methoxy-5-trifluoromethoxybenzyl)amino-2-phenylpiperidine (CP-122,721)[21] were shown to reduce symptoms of depression in phase II studies, this could not be confirmed for aprepitant in a phase III trial.[22] Several NK_1 receptor antagonists are currently in clinical development for depression and other psychiatric disorders, such as anxiety.[22] Moreover, recent results from two randomized, double-blind, placebo-controlled phase II studies with the novel NK_1 antagonist (2*R*,4*S*)-4-(4-acetyl-1-piperazinyl)-*N*-[(1*R*)-1-[3,5-bis(trifluoromethyl)phenyl]ethyl]-2-(4-fluoro-2-methylphenyl)-*N*-methyl-1-piperidinecarboxamide (casopitant, GW 679769)[23] in patients with major depressive disorder suggest that NK_1 antagonists with nearly complete receptor occupancy could be effective in the treatment of depression.[24] On the basis of this evidence, it can be hypothesized that the combination of NK_3 and NK_1 receptor antagonism may provide a therapeutic benefit for positive, negative, and mood symptoms associated with schizophrenia.

(2*R*,3*S*)-2-(3,5-Bis-trifluoromethylphenyl)-*N*-[4-(4-fluoro-2-methylphenyl)-6-(3-hydroxy-2-hydroxymethylpyrrolidin-1-yl)-pyridin-3-yl]-*N*-methylisobutyramide (RO4583298)[25] is a novel NK_1/NK_3 antagonist that binds with high affinity to hNK_1 (K_i = 0.7 nM) and hNK_3 (K_i = 2.9 nM). Its in vitro and in vivo characterization has demonstrated that it had an insurmountable (also referred as apparent noncompetitive or pseudo-irreversible[26]) and long-lasting mode of antagonism at both hNK_1 and hNK_3.[27] Compound **5** (RO4583298) robustly blocked the gerbil foot tapping response in a dose-dependent manner with an ED_{50} of 0.4 mg/kg (po) and with a long-lasting in vivo effect. Remarkably, this long-lasting in vivo receptor blockade by compound **5** coincided well with its insurmountable mode of antagonism observed in vitro.[27] Recently, researchers at GSK have reported novel dual NK_1/NK_3 antagonists based on a similar pyridine scaffold as compound **5**.[28,29] Interestingly, among these compounds, 2-[3,5-bis-(trifluoromethyl)phenyl]-*N*-{4-(4-fluoro-2-methylphenyl)-6-[(4-(hydroxymethyl)-1-methyl-5-oxo-3-pyrrolidinyl]-3-pyridinyl}-*N*,2-dimethylpropanamide (enantiomer 2) (GSK, "compound **17a**")[28,29] has a high structural similarity to compound **5** and differs only in the pyrrolidine substituent (Figure 1). Compound **17a** was reported to have a high potency at NK_1 (K_i = 0.06 nM) and NK_3 (K_i = 1 nM), as measured in a functional cell-based assay, and also displayed an insurmountable profile of antagonism at both NK_1 and NK_3.[29]

The objective of the current study was to elucidate the molecular interaction between human NK_1/NK_3 and compound **5**, which is involved in the slow kinetics and insurmountable behavior at both receptors. Using site-directed mutagenesis, rhodopsin-based hNK_1 and hNK_3 modeling, and functional [^{3}H]IP accumulation assay, we have identified a single amino acid in the helix position 6.51 of both NK_1 and NK_3 as a crucial residue that determines the insurmountable behavior of compound **5**. We then hypothesized that the hydroxymethyl ($-CH_2OH$) group of compound **5** was needed for this insurmountable behavior. The antagonism modes of six close analogues with or without $-CH_2OH$ group were further analyzed, and the results have strengthened our hypothesis.

RESULTS

Inhibition Mode of NK Antagonists on the SP- or [MePhe^7]NKB-Evoked Accumulation of [^{3}H]IP at Human NK_1 and NK_3 Receptors. Compound **5** and its derivative (*S*)-2-(3,5-bis-trifluoromethylphenyl)-*N*-[4-(4-fluoro-2-methylphenyl)-6-((*S*)-4-methanesulfonyl-3-methylpiperazin-1-yl)-pyridin-3-yl]-*N*-methylisobutyramide (RO4908594), which originated from an internal drug discovery program,[25] belong to a novel structural class binding to both NK_1 and NK_3. Their chemical structures are different from those of selective antagonists of NK_1 **1** (aprepitant) and (2*S*,3*S*)-*cis*-2-(diphenylmethyl)-*N*-[(2-methoxyphenyl)methyl]-1-azabicyclo[2.2.2]-octan-3-amine (CP-96,345)[30] and of NK_3 **3** (osanetant) and **4** (Figure 1). The biochemical characterization of compounds **5**

dx.doi.org/10.1021/jm2017072 | *J. Med. Chem.* 2012, 55, 5061−5076

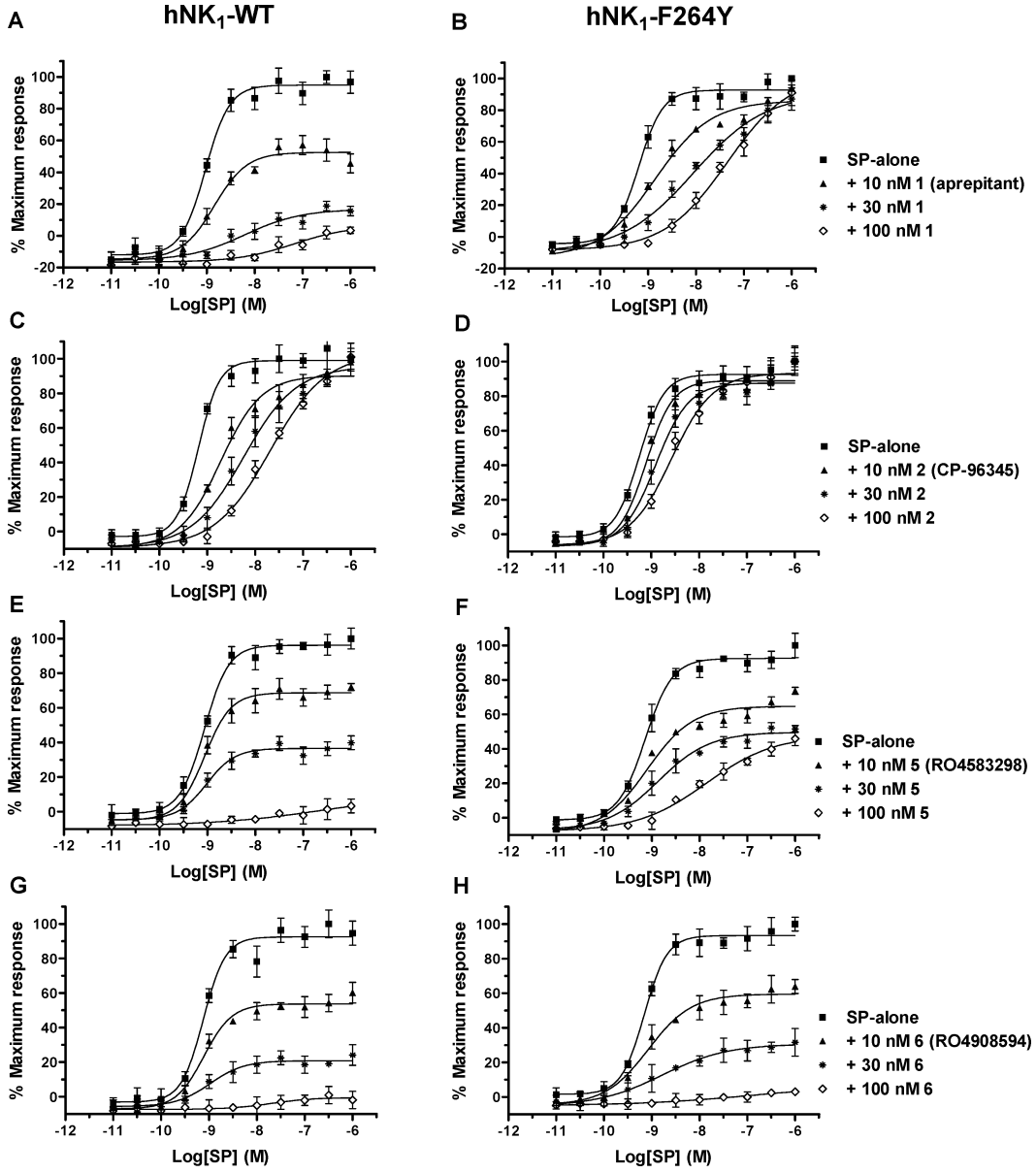

Figure 2. Schild plot analyses for antagonism of SP-induced accumulation of [^{3}H]IP by compounds **1**, **2**, **5**, and **6**: concentration−response curves for [^{3}H]IP formation stimulated by SP in the absence and presence of various concentrations of compound **1** (A, B), compound **2** (C, D), compound **5** (E, F), and compound **6** (G, H) in HEK293 cells expressing transiently the hNK$_1$-WT or hNK$_1$-F264Y[6,51]. Each curve represents the mean of six concentration−response measurements from three independent transfections.

and **6** (RO4908594) has been previously described.[27,31] To compare the inhibition mode of **5**, **6**, and selective NK$_1$ and NK$_3$ antagonists for NK$_1$ and NK$_3$, we measured the concentration−response curves (CRCs) for [^{3}H]IP formation stimulated by SP (NK$_1$ agonist) or [MePhe^7]NKB (NK$_3$ agonist) in the absence or presence of increasing concentrations of antagonist in HEK293 cells transiently transfected with various NK receptors. In the hNK$_1$ expressing cells, SP elicited concentration-dependent increases in the accumulation of [^{3}H]IP with the EC$_{50}$ of 0.6 ± 0.0 nM. Consistent with a previous report,[19] compound **1** displayed an insurmountable mode of antagonism at hNK$_1$, shifting SP CRCs to the right with a concomitant decrease in maximal response (Figure 2A and Table 1), whereas compound **2** (CP-96,345)[30] behaved as a surmountable antagonist at hNK$_1$, shifting the SP CRCs to the right without changing its maximal response (Figure 2C, and pA_2 and Schild slope values shown in Table 1). Both compounds **5** and **6** also behaved as insurmountable antagonists at hNK$_1$, producing a rightward shift in SP CRC as well as a full suppression of the maximal response (Figure 2E,G and Table 1).

[MePhe^7]NKB was used as agonist because it has been shown to have a high selectivity for hNK$_3$ (K_i = 0.3 nM) versus hNK$_2$ (K_i = 1597 nM) and hNK$_1$ (K_i > 10000 nM).[6] [MePhe^7]NKB elicited concentration-dependent increases in the accumulation of [^{3}H]IP in HEK293 cells expressing hNK$_3$ with an EC$_{50}$ of 0.71 ± 0.0 nM. Compound **5** displayed an insurmountable mode of antagonism at the hNK$_3$ receptor (Figure 3C and Table 2), while compound **6** behaved in a surmountable manner at hNK$_3$ (Figure 3E and Table 2). Both compounds **3** and **4** behaved as surmountable antagonists at hNK$_3$, shifting the NKB CRC to the right without changing its

dx.doi.org/10.1021/jm2017072 | J. Med. Chem. 2012, 55, 5061−5076

Table 1. Schild Analyses for the Antagonism of SP-Induced Accumulation of [^{3}H]IP by Selective NK_1 and Dual NK_1/NK_3 Antagonists in HEK293 Cells Expressing Transiently the hNK_1-WT or hNK_1-F264Y$^{6.51}$ [a]

	SP-induced [^{3}H]IP accumulation					
	hNK_1-WT			hNK_1-F264Y$^{6.51}$		
NK antagonist	pA_2	Schild slope	mode of antagonism	pA_2	Schild slope	mode of antagonism
1	ND	ND	insurmountable	8.08	1.76	surmountable
2	8.27	1.19	surmountable	7.78	0.98	surmountable
5	ND	ND	insurmountable	7.54	2.24	partial insurmountable
7	ND	ND	insurmountable	7.40	2.43	partial insurmountable
9	ND	ND	insurmountable	7.77	2.69	partial insurmountable
8	ND	ND	insurmountable	ND	ND	insurmountable
6	ND	ND	insurmountable	ND	ND	insurmountable
10	ND	ND	insurmountable	ND	ND	insurmountable
11	ND	ND	insurmountable	ND	ND	insurmountable

[a]The apparent antagonist potency (pA_2, −log of the molar concentration of antagonist producing a 2-fold shift of the concentration response curve) and Schild slope values of antagonists at hNK_1-WT and hNK_1-F264Y$^{6.51}$ were determined using SP CRCs in the absence and presence of various concentrations of antagonist and Schild plot analyses. ND, not determined.

maximal response (Figure 3A and pA_2 and slope values shown in Table 2).

To explore which structural elements determine the antagonistic mode of action of compounds **5** and **6** at NK_1 and NK_3, the five derivatives **7**, **8**, **9**, **10**, and **11** (Figure 4) were further investigated in the SP- or NKB-induced formation of [^{3}H]IP assay in HEK293 cells transiently expressing hNK_1 and hNK_3. Compounds **7**−**11** are dual NK_1/NK_3 antagonists,[25] and their selection was guided by our docking model that predicted the hydroxymethyl group on compounds **5**, **7**, and **9** to be involved in the insurmountable mode of antagonism at NK_3. All five antagonists **7**−**11** had an insurmountable profile at hNK_1 (Table 1). As predicted, compounds **5**, **7**, and **9** acted in an insurmountable manner at hNK_3 (Figure 3C,G and Table 2), while compounds **8**, **10**, and **11** displayed a surmountable mode of antagonism at hNK_3 (pA_2 and slope values shown in Table 2).

Mutant Selection. Comparing the structure of the two NK_1/NK_3 antagonists **5** and **6**, we concluded that the difference in their kinetic behavior should be caused by interactions of the amine substituents with the receptor. These substituents are predicted by the model to be located in the pocket formed by residues of the TMDs 3, 5, and 6. Important in terms of binding energy, it struck us that compound **5** with its $-CH_2OH$ group may form a hydrogen bond with the OH group of hNK_3-Tyr315$^{6.51}$ while compound **6** cannot form a hydrogen bond with the phenolic OH. Normally, hydrogen bond donors without any interaction partner should cause a loss of binding energy and, if this hypothesis is correct, the mutation hNK_3-Y315F$^{6.51}$ should lead to an insurmountable behavior of compound **6**. This would also fit the fact that both compounds are insurmountable at hNK_1, which has Phe264$^{6.51}$. In analogy, we also investigated the mutation hNK_1-F264Y$^{6.51}$ with the expectation that compound **6** should then become surmountable.

In order to get additional validation of this hypothesis from the ligand side, we tested the five structurally closely related compounds **7**−**11** on these mutations, as well as two NK_1 selective antagonists and two NK_3 selective antagonists.

Depending on the exact conformation of His$^{6.52}$, the $-CH_2OH$ group could alternatively bind to a nitrogen of this side chain. Also, the −OH function could bind to the phenolic OH of Tyr$^{5.38}$. Although these residues are conserved between hNK_1 and hNK_3, and thus these interactions would not explain the different kinetics of compound **6** at the two receptors, we also included them in the mutation studies to further validate our hypothesis.

Effect of the Mutation at Helix Position 6.51 on Antagonism Mode of NK Antagonists. An alignment of the amino acids in the seven-transmembrane domain (7TMD) forming the NK receptor binding pockets toward the 7TMD of bovine rhodopsin (PDB code 1F88)[32] and human β2-adrenergic receptor (PDB code 2RH1)[33,34] is shown in Figure 5. The only amino acid difference in TM6 between hNK_1 and hNK_3 is the residue Phe264$^{6.51}$ in hNK_1, which corresponds to Tyr315$^{6.51}$ in hNK_3 (Figure 5). Our docking models of NK_1 and NK_3 predicted that the residue at helix position 6.51 might contribute to the mode of antagonism of NK antagonists. Hence, hNK_1-Phe264$^{6.51}$ was converted to Tyr264$^{6.51}$ and and hNK_3-Tyr315$^{6.51}$ to Phe315$^{6.51}$. Since the mutation hNK_1-F264Y$^{6.51}$ had no effect on SP potency and the mutation hNK_3-Y315F$^{6.51}$ had a minor effect on [MePhe^7]NKB potency, the antagonism modes of compounds **1**−**11** were compared at the mutated hNK_1-F264Y$^{6.51}$ and hNK_3-Y315F$^{6.51}$ receptors using Schild analyses. As seen, the mutation hNK_1-F264Y$^{6.51}$ converted compound **1** from insurmountable to surmountable (Figure 2B and Table 1) and compounds **5**, **7**, and **9** from insurmountable to partially insurmountable (Figure 2F and Table 1) and had no effect on antagonism modes of compounds **2**, **6**, **8**, **10**, **11** (Figure 2D,H and Table 1). Conversely, hNK_3-Y315F$^{6.51}$ converted compound **6** from a surmountable to an insurmountable antagonist (Figure 3F and Table 2), while it had no effect on the modes of antagonism of compounds **3**, **4**, **8**, **10**, and **11** except for increasing their potency (Figure 3B and Table 2). For compounds **5**, **7**, and **9** the mutation hNK_3-Y315F$^{6.51}$ caused a further depression in maximal NKB response at a compound concentration of 10 nM (Figure 3D,H and Table 2).

Effect of the Mutation at Helix Position 6.51 on Binding Affinity of NK Antagonists As Measured by Displacement Studies. The affinity constants of NK antagonists in the membrane preparations from HEK293 cells transiently expressing hNK_1-WT, hNK_1-F264Y, hNK_3-WT, or hNK_3-Y315F are given in Table 3. The affinity constants of compounds **1** and **2** were not affected by mutation hNK_1-F264Y (Figure 6A,B and Table 3). The mutation hNK_3-Y315F led to an increase in the K_i of compound **3** by 18-fold (P = 0.0006), yet caused an increase in affinity of compound **4**

dx.doi.org/10.1021/jm2017072 | J. Med. Chem. 2012, 55, 5061−5076

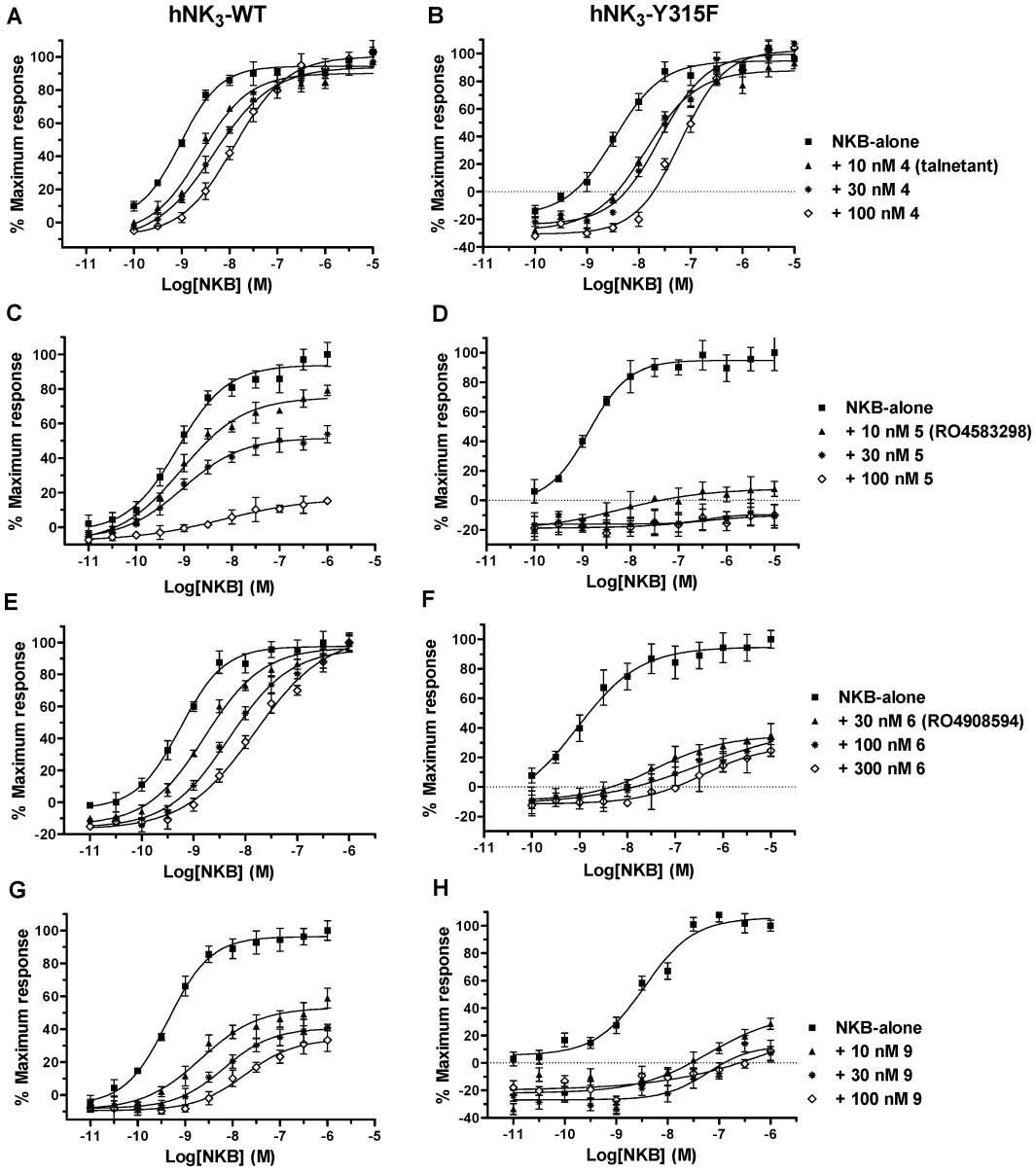

Figure 3. Schild plot analyses for antagonism of [MePhe^7]NKB-induced accumulation of [^{3}H]IP by compounds **4**, **5**, **6**, and **9**: concentration−response curves for [^{3}H]IP formation stimulated by [MePhe^7]NKB in the absence and presence of various concentrations of compound **4** (A, B), compound **5** (C, D), compound **6** (E, F), and compound **9** (G, H) in HEK293 cells expressing transiently the hNK$_3$-WT or hNK$_3$-Y315F$^{6.51}$. Each curve represents the mean of six concentration−response measurements from three independent transfections.

by a factor of 2.1 (P = 0.012) (Figure 6C,D and Table 3). As seen in Figure 6 and Table 3, both compounds **5** and **6** bind with similar affinity to hNK$_1$-WT and hNK$_1$-F264Y, but their affinities were increased for mutation hNK$_3$-Y315F by 4.1- and 8.5-fold (statistical significance of P = 0.0019 and P = 0.0063), respectively, in comparison to the WT. Similarly, the mutation hNK$_1$-F264Y did not affected the affinity constants of compounds **7**−**11**, while the mutation hNK$_3$-Y315F caused increases in affinities of compounds **7**−**11** that were statistically significant (Table 3).

Effect of the Mutations at Helix Positions 5.38 and 6.52 of NK$_3$ Receptor on Antagonism Mode and Binding Affinity of NK Antagonists. To investigate the role of hNK$_3$ residues at helix positions 5.38 and 6.52 on the mode of antagonism of NK antagonists, the NKB-induced formation of [^{3}H]IP was tested in HEK293 cells expressing transiently the WT and mutated hNK$_3$ receptors. The EC$_{50}$, n_H, and relative E_{max} values, calculated from concentration−response curves of [MePhe^7]NKB, are given in Table 4. NKB was completely unable to evoke accumulation of [^{3}H]IP in HEK293 cells transiently expressing the NK$_3$ mutants: Y247A$^{5.38}$, Y247W$^{5.38}$, and H316F$^{6.52}$. Except for a decrease in efficacy of NKB at mutant Y247F$^{5.38}$ (relative E_{max} was decreased by 46%), the mutations Y247F$^{5.38}$ and H316W$^{6.52}$ had no effect on the potency of NKB-induced accumulation of [^{3}H]IP (Table 4). Therefore, the mutants Y247F$^{5.38}$ and H316W$^{6.52}$ were further chosen to study the antagonism modes of compounds **3**, **4**, **5**, and **6** by Schild analyses. The Schild constants (pA_2 values and Schild slope) for antagonism of NKB-induced accumulation of [^{3}H]IP by compounds **3**, **4**, **5**, and **6** in HEK293 cells expressing hNK3-WT, Y247F$^{5.38}$, or H316W$^{6.52}$ are given in Table 5. The mutation Y247F$^{5.38}$ had no effect on the surmountable antagonism mode of compounds **3**, **4**, and **6** or on the insurmountable mode of compound **5**. Except for a decrease in

dx.doi.org/10.1021/jm2017072 | J. Med. Chem. 2012, 55, 5061−5076

Table 2. Schild Analyses for the Antagonism of [MePhe^7]NKB-Induced Accumulation of [^{3}H]IP by Selective NK_3 and Dual NK_1/NK_3 Antagonists in HEK293 Cells Expressing Transiently the hNK_3-WT or hNK_3-Y315F$^{6.51}$ [a]

	[MePhe^7]NKB-induced [^{3}H]IP accumulation					
	hNK_3-WT			hNK_3-Y315F$^{6.51}$		
NK antagonist	pA_2	Schild slope	mode of antagonism	pA_2	Schild slope	mode of antagonism
3	7.73	1.59	surmountable	7.53	0.96	surmountable
4	8.24	0.88	surmountable	8.63	0.76	surmountable
5	ND	ND	insurmountable	ND	ND	more insurmountable
7	ND	ND	insurmountable	ND	ND	more insurmountable
9	ND	ND	insurmountable	ND	ND	more insurmountable
8	6.92	0.7	surmountable	7.68	0.71	surmountable
6	7.79	1.12	surmountable	ND	ND	insurmountable
10	6.91	0.63	surmountable	8.61	2.00	surmountable
11	7.01	0.61	surmountable	7.43	1.2	surmountable

[a]The apparent antagonist potency (pA_2) and Schild slope values of antagonists at hNK_3-WT and hNK_3-Y315F$^{6.51}$ were determined using NKB CRCs in the absence and presence of various concentrations of antagonist and Schild plot analyses. ND, not determined.

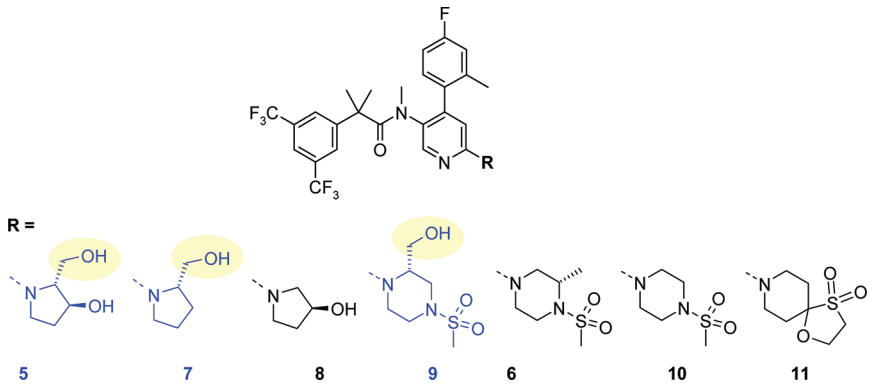

Figure 4. Chemical structures of the dual NK_1/NK_3 antagonists, 2-phenyl-*N*-(pyridin-3-yl)-*N*-methylisobutyramide derivatives, compounds **5**–**11**. The group that controls the mode of antagonism is indicated by a yellow highlighted circle.

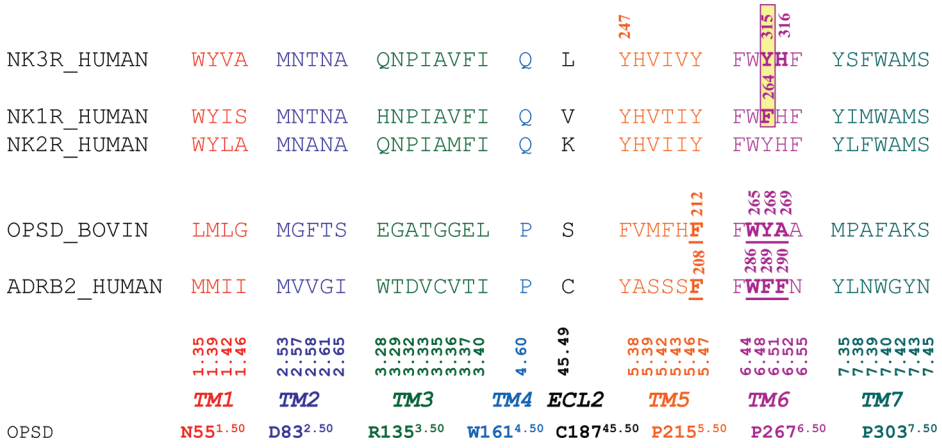

Figure 5. Alignment of the amino acids forming the binding site of NK_1, NK_2, and NK_3 toward the 7TMD of bovine rhodopsin (PDB code 1F88)[32] and human β2-adrenergic (PDB code 2RH1)[33,34] receptors. The Ballesteros–Weinstein numbering scheme of the amino acids[47] are given to facilitate the comparison with other GPCRs (see Experimental Section). The conserved residue in each TM of rhodopsin that is assigned as 50 is shown in the bottom row. The numbers above the NK3R_HUMAN and NK1R_HUMAN receptors give the sequence number of the position of the mutation carried out in this study. The residue at helix position 6.51, which is different between NK_1 and NK_3 binding pockets, is boxed and yellow highlighted. Four residues at helix positions 5.47, 6.48, 6.51, and 6.52 that have been shown in the high resolution X-ray structures to be involved in the toggle switch mechanism of hβ2AR activation[33,34] and bovine rhodopsin activation[32] are indicated in bold underlined with their amino acid sequence number shown above.

potency of compound **4**, the mutation of H316W$^{6.52}$ had no effect on the mode of antagonism of compounds **3** and **4**, but it completely abolished the ability of compounds **5** and **6** to shift NKB CRC to the right (Table 5).

To characterize the binding properties of the hNK_3 mutants at helix positions 5.38 and 6.52, the saturation isotherm and competition binding analyses were performed at binding equilibrium using radioligand [^{3}H]**3** ([^{3}H]SR 142801) on

dx.doi.org/10.1021/jm2017072 | J. Med. Chem. 2012, 55, 5061–5076

Table 3. Radioligand Binding Affinity of NK Antagonists in Membrane Preparations from HEK293 Cells Transiently Expressing hNK$_1$-WT, hNK$_1$-F264Y$^{6.51}$, hNK$_3$-WT, or hNK$_3$-Y315F$^{6.51}$ [a]

	[^{3}H]SP competition binding				[^{3}H]**3** competition binding				
	hNK$_1$-WT		hNK$_1$-F264Y$^{6.51}$		hNK$_3$-WT		hNK$_3$-Y315F$^{6.51}$		
NK antagonist	K_i, nM	n_H	K_i, nM	n_H	K_i, nM	n_H	K_i, nM	fold affinity increase	n_H
1	03 ± 0.0	1.1 ± 0.0	0.8 ± 0.1	0.8 ± 0.1	454.1 ± 66.1	1.0 ± 0.1	ND	ND	ND
2	0.4 ± 0.2	0.5 ± 0.0	0.3 ± 0.4	0.9 ± 0.3	>10,000		ND	ND	ND
3	209.6 ± 24.6	0.9 ± 0.2	ND	ND	0.6 ± 0.1	1.1 ± 0.0	10.8 ± 0.8	0.06***	0.9 ± 0.1
4	>10000		ND	ND	3.6 ± 0.7	1.0 ± 0.0	1.7 ± 0.4	2.1*	1.0 ± 0.1
5	0.7 ± 0.1	1.0 ± 0.1	1.1 ± 0.2	0.7 ± 0.1	2.9 ± 0.3	1.1 ± 0.1	0.7 ± 0.1	4.1**	1.1 ± 0.2
7	1.4 ± 0.3	0.9 ± 0.06	2.8 ± 0.9	1.8 ± 0.4	1.5 ± 0.2	1.1 ± 0.07	0.6 ± 0.1	2.5*	1.2 ± 0.09
9	0.7 ± 0.2	1.1 ± 0.05	1.3 ± 0.1	2.4 ± 0.5	1.2 ± 0.2	1.1 ± 0.02	0.6 ± 0.1	2*	1.5 ± 0.1
8	1.3 ± 0.4	1.0 ± 0.05	2.1 ± 0.3	1.9 ± 0.1	11.9 ± 1.1	1.1 ± 0.04	2.5 ± 0.4	4.8**	1.0 ± 0.04
6	0.3 ± 0.1	0.7 ± 0.1	0.5 ± 0.4	1.6 ± 0.1	1.7 ± 0.3	1.1 ± 0.0	0.2 ± 0.0	8.5**	1.2 ± 0.1
10	0.4 ± 0.1	0.8 ± 0.04	1.4 ± 0.1	1.8 ± 0.1	2.4 ± 0.37	1.0 ± 0.04	0.7 ± 0.01	3.4**	1.1 ± 0.02
11	1.4 ± 0.3	1.0 ± 0.1	1.7 ± 0.2	1.5 ± 0.1	3.5 ± 0.3	1.3 ± 0.15	1.0 ± 0.2	3.5**	1.2 ± 0.08

[a]The affinity constant (K_i) and Hill slope (n_H) values for various NK antagonists determined using either [^{3}H]SP or [^{3}H]**3** were calculated as described in the Experimental Section. Radioligands concentrations were the following: 0.3 and 0.8 nM [^{3}H]SP for hNK$_1$-WT and hNK$_1$-F264Y$^{6.51}$ membranes, respectively; 0.2 and 1.8 nM [^{3}H]**3** for hNK$_3$-WT and hNK$_3$-Y315F$^{6.51}$ membranes, respectively. Values are the mean ± SE of the K_i and were calculated from three independent experiments, each performed in duplicate. Statistical significance was determined using a two-tailed unpaired Student's t test: (*) $P < 0.05$, (**) $P < 0.01$, (***) $P < 0.001$. ND, not determined.

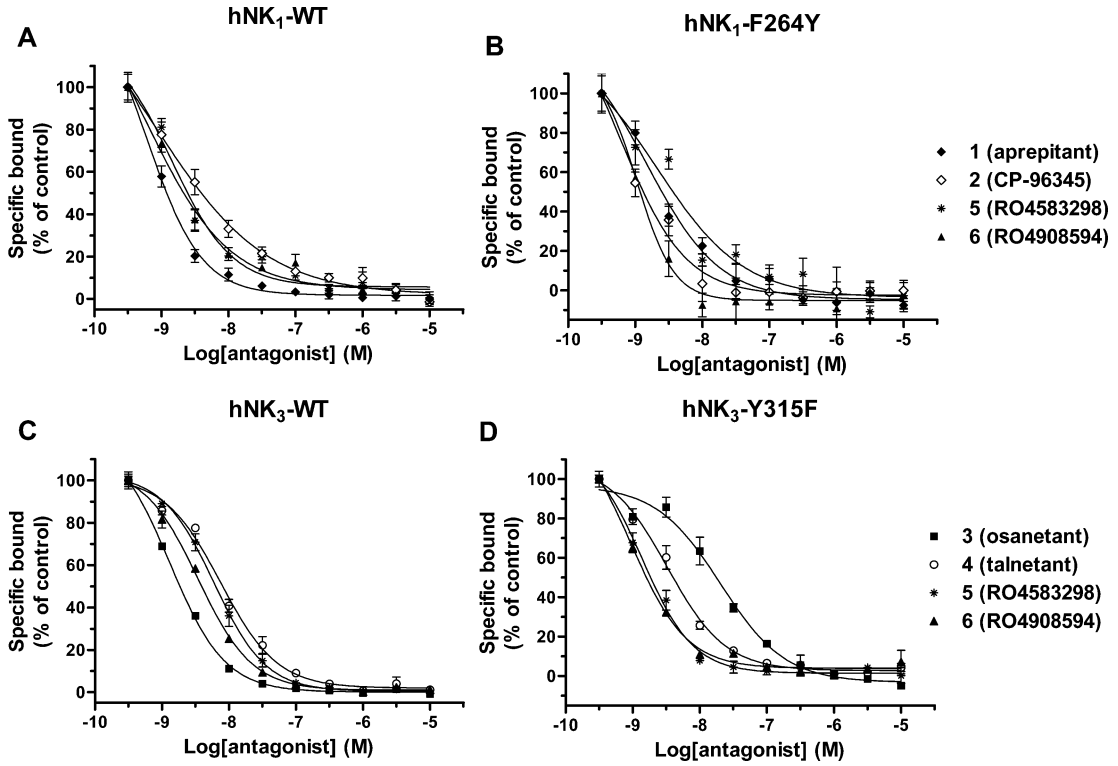

Figure 6. Effects of the mutation at helix position 6.51 on the competition binding of compounds **1**, **2**, **3**, **4**, **5**, and **6** in membrane preparations from HEK293 cells transiently expressing hNK$_1$-WT (A), hNK$_1$-F264Y$^{6.51}$ (B), hNK$_3$-WT (C), or hNK$_3$-Y315F$^{6.51}$ (D). The [^{3}H]SP and [^{3}H]**3** at concentrations equal to their K_D values were used in these competition binding experiments. Each data point is the mean ± SE (bars) of three individual experiments performed in duplicate.

membranes isolated from HEK293 cells transiently transfected with hNK$_3$-WT and mutated receptors. The dissociation constants (K_D) and the maximum number of binding sites (B_{max}) derived from the saturation isotherms of [^{3}H]**3** at hNK$_3$-WT and mutated receptors are given in Table 6. The binding affinity of [^{3}H]**3** was lost at mutant Y247A$^{5.38}$. The mutation H316W$^{6.52}$ caused decreases in the binding affinity of [^{3}H]**3** by 11.0-fold ($P = 0.01$), while the mutations Y247F$^{5.38}$, Y247W$^{5.38}$, and H316F$^{6.52}$ had no effect on the K_D values of [^{3}H]**3** (Table 6). Therefore, four mutations Y247F$^{5.38}$, Y247W$^{5.38}$, H316F$^{6.52}$, and H316W$^{6.52}$, which did not affect or only partially affected the binding affinity of [^{3}H]**3**, were chosen further for the competition binding studies with compounds **3**, **4**, **5**, and **6**. Table 6 summarizes the affinity constant (K_i) and Hill slope (n_H) values for the [^{3}H]**3** displacement by **3**, **4**, **5**, or **6** on HEK293 cell membranes expressing four point-mutated hNK$_3$.

dx.doi.org/10.1021/jm2017072 | J. Med. Chem. 2012, 55, 5061–5076

Table 4. Effect of Mutation on the [MePhe^7]NKB-Evoked Accumulation of [^{3}H]IP^a

		[MePhe^7]NKB		
hNK$_3$	position in 7TMD	EC$_{50}$, nM	n_H	relative E_{max}
WT		0.71 ± 0.04	0.8 ± 0.0	100
Y247F	5.38	2.22 ± 1.08	0.7 ± 0.0	46.37 ± 5.17
Y247A	5.38	inactive	inactive	inactive
Y247W	5.38	inactive	inactive	inactive
H316F	6.52	inactive	inactive	inactive
H316W	6.52	3.48 ± 1.61	0.9 ± 0.0	146.32 ± 4.55

^{a}EC$_{50}$, Hill slope (n_H), and relative efficacy (E_{max}) values for the NKB-induced formation of [^{3}H]IP in HEK293 cells expressing transiently the WT or mutated NK$_3$ receptors. The data are the mean ± SE of eight concentration−response measurements (each performed in duplicate) from four independent transfections.

In the competition binding experiments by compounds **3**−**6** (Figure 7 and Table 6), the mutation Y247F$^{5.38}$ had no effect on the competition bindings by compounds **3**−**6**. The mutation Y247W$^{5.38}$ decreased only the binding affinity of compound **4** by 10.3-fold (statistical significance of P = 0.03). H316F$^{6.52}$ caused only a decrease in binding affinity of compound **6** by 11.6-fold (statistical significance of P = 0.0035), while the mutation H316W$^{6.52}$ caused decreases in binding affinities of compounds **3**, **4**, **5**, and **6** by 8.0-, 33.9-, 693.1-, and >10000-fold (statistical significance of P of 0.01, 0.0002, 0.0001, and <0.0001), respectively. In general, there was a good agreement between the functional [^{3}H]IP accumulation (Table 5) and competition binding results (Table 6) for compounds **3**−**6** at mutants Y247F and H316W.

DISCUSSION AND CONCLUSION

In the current study, the −CH$_2$OH substituted compounds **5**, **7**, and **9** exhibited an insurmountable mode of antagonism at both hNK$_1$ and hNK$_3$. This mode of action was characterized by a parallel rightward shift of the SP or [MePhe^7]NKB concentration−response curves (increase in EC$_{50}$ values) in the presence of increasing antagonist concentration, with a concomitant large decrease in the maximal agonist-evoked response (E_{max}). A possible explanation for this insurmountable antagonism of compounds **5**, **7**, and **9** at NK$_1$ and NK$_3$ determined by Schild plot analyses might be their slow dissociation rate from NK$_1$ and NK$_3$. Consequently, a large portion of the NK$_1$ and NK$_3$ receptors are not available for activation by SP or [MePhe^7]NKB and, thereby, the maximally achievable response of SP or [MePhe^7]NKB drops dramatically in comparison to the fast dissociating surmountable antagonist.[35] In contrast, compounds **6**, **8**, **10**, and **11** lacking the −CH$_2$OH group had an insurmountable profile at hNK$_1$, but all had a surmountable mode of antagonism at hNK$_3$ (parallel rightward shifts of agonist dose−response curves with no alteration of E_{max}). To better understand the different behavior of compounds **5** and **6**, we looked at the docking of these compounds onto the NK$_1$- and NK$_3$-7TMD binding cavities (Figure 8). The docking modes suggested several mutations that might be relevant for the different behavior of the compounds investigated in this study.

In agreement with our hypothesis, we identified hNK$_3$-Tyr$^{6.51}$ as a contributing cause for the different modes of antagonism of compounds **5** and **6**. The mutation hNK$_3$-Y315F$^{6.51}$ converted the surmountable mode of antagonism of compound **6** to an insurmountable one, indicating that the presence of the OH function of hNK$_3$-Tyr$^{6.51}$ is plausibly the reason for the difference between hNK$_1$ and hNK$_3$. This goes in parallel with the 8.5-fold increase of binding affinity through this mutation. The same mutation led to an even stronger insurmountable mode of antagonism of compound **5** compared to the hNK$_3$-WT and to a 4.1-fold increase in binding affinity. The observed effect of this mutation on compound **6** agrees with our hypothesis. However, for compound **5**, on the basis of our hypothesis, we would have expected at first that this mutation would lead to a decrease of the insurmountable mode of antagonism. A possible explanation why it is not the case might be that the formation of the hydrogen bond between a phenolic OH and an aliphatic OH is not as favorable as the presence of a coordinatively unsaturated aliphatic OH group in the ligand, possibly as consequence of a high desolvation penalty of the phenolic OH when it binds to the ligand's alcoholic OH group or that the alcoholic OH group can then interact with another hydrogen bonding partner such as, for example, a water molecule. In any case, hNK$_3$-Y315F$^{6.51}$ seems to represent a preferred energetic situation. Nevertheless, the hypothesis described above is only one among other possible explanations for this observation. The experimental results agree with our hypothesis that the Y$^{6.51}$F difference between the hNK$_1$ and hNK$_3$ receptors is responsible for the different antagonism modes of compounds **5** and **6**. In this context, it is interesting to note that compound **17a** (GSK), which exhibited an insurmountable mode of antagonism at NK$_1$/NK$_3$, also contains a −CH$_2$OH group, just like compound **5**.[29]

To further test the importance of the −CH$_2$OH group, we also included compounds **7**, **8**, **9**, **10**, and **11** in our study. As expected, the −CH$_2$OH substituted compound **7** was also insurmountable at hNK$_3$ while compounds **8**, **10**, and **11** lacking this functional group displayed a surmountable mode of antagonism. Most remarkable was the result that the hybrid structure compound **9** behaved indeed as insurmountable antagonist at hNK$_3$. Thus, we have identified the presence of an alcoholic function in the ligand as trigger that renders the pyridine series insurmountable at hNK$_3$, possibly by the

Table 5. Schild Constants for Antagonism of [MePhe^7]NKB-Induced Accumulation of [^{3}H]IP by Compounds 3, 4, 5 and 6 in HEK293 Cells Expressing Transiently the hNK$_3$-WT and Mutants^a

		3			4				6		
hNK$_3$	position in 7TMD	pA_2	Schild Slope	mode of antagonism	pA_2	Schild Slope	mode of antagonism	**5**, mode of antagonism	pA_2	Schild Slope	mode of antagonism
WT		7.73	1.59	surmountable	8.24	0.88	surmountable	insurmountable	7.79	1.12	surmountable
Y247F	5.38	8.23	0.94	surmountable	8.54	0.84	surmountable	insurmountable	7.32	2.73	surmountable
H316W	6.52	7.77	1.13	surmountable	6.64	1.14	surmountable	inactive	inactive	inactive	inactive

^{a}The apparent antagonist potency (pA_2) and Schild slope values of compounds **3**, **4**, and **6** at hNK$_3$-WT and mutants were determined from NKB CRCs in the absence and presence of various concentrations of antagonist and Schild plot analyses.

dx.doi.org/10.1021/jm2017072 | J. Med. Chem. 2012, 55, 5061−5076

Table 6. Effect of the Mutations on Binding Properties of Compound 3 and on the Binding Constants (K_i) of Compounds 3, 4, 5, and 6 As Measured by Saturation Binding Isotherms and Competition Binding Assay Using [^{3}H]3 in Membrane Preparations from HEK293 Cells Transiently Transfected with the WT and Mutated hNK$_3$ As Described in Experimental Section[a]

	[^{3}H]3 saturation analysis			[^{3}H]3 competition binding												
				3			4			5			6				
hNK$_3$	K_D, nM	K_D(mut)/K_D(WT)	B_{max}, pmol/(mg prot)	K_i, nM	K_i(mut)/K_i(WT)	n_H	K_i, nM	K_i(mut)/K_i(WT)	n_H	K_i, nM	K_i(mut)/K_i(WT)	n_H	K_i, nM	K_i(mut)/K_i(WT)	n_H	
WT	0.2 ± 0.0		8.0 ± 0.3	0.6 ± 0.1		1.1 ± 0.0	3.6 ± 0.7		1.0 ± 0.0	2.9 ± 0.3		1.1 ± 0.1	1.7 ± 0.3		1.1 ± 0.0	
Y247F	0.7 ± 0.3	3.5	5.9 ± 0.6	0.5 ± 0.4	0.8	0.8 ± 0.1	3.7 ± 0.1	1.0	1.0 ± 0.1	3.9 ± 0.1	1.3	1.0 ± 0.0	1.8 ± 0.3	1.1	1.1 ± 0.1	
Y247A	NDB	NDB	NDB	CNM	CNM	CNM	CNM	CNM	CNM	CNM	CNM	CNM	CNM	CNM	CNM	
Y247W	1.0 ± 0.2	5.0	2.6 ± 0.5	2.1 ± 0.7	3.5	1.1 ± 0.0	37.2 ± 6.3	10.3*	0.9 ± 0.1	3.4 ± 0.9	1.2	0.9 ± 0.0	5.1 ± 1.1	3.0	0.7 ± 0.1	
H316F	0.08 ± 0.0	0.4	14.8 ± 0.8	0.4 ± 0.2	0.7	1.2 ± 0.0	10.6 ± 1.3	2.9	0.92 ± 0.1	12.5 ± 1.3	4.3	1.1 ± 0.1	19.7 ± 3.1	11.6**	1.0 ± 0.0	
H316W	2.2 ± 0.4	11.0*	24.3 ± 2.2	4.8 ± 1.3	8.0*	1.3 ± 0.1	122.0 ± 9.0	33.9***	1.1 ± 0.2	2010 ± 720.0	693.1***	1.7 ± 0.4	>10000			

[a]The K_D and B_{max} values are the mean ± SE, calculated from three independent experiments (each performed in triplicate). The K_i values are mean ± SE calculated from three independent experiments, each performed in duplicate. The mutations that affected the affinity of antagonists in comparison to WT are shown in boldface type. Statistical significance was determined using a two-tailed unpaired Student's t test: (*) $P < 0.05$, (**) $P < 0.01$, (***) $P < 0.001$. NDB, no detectable binding because of high nonspecific binding. CNM, cannot be measured because of loss of binding affinity of [^{3}H]3.

formation of a hydrogen bond between hNK$_3$-Tyr$^{6.51}$ and the hydroxy group of the ligand. While compounds **7** and **9** also showed the expected strengthening of their insurmountable behavior at mutation hNK$_3$-Y315F$^{6.51}$, compounds **8**, **10**, and **11** stayed surmountable at mutation hNK$_3$-Y315F$^{6.51}$, yet with large increases in their pA_2 values and binding affinities. This shows that for these compounds removal of the $-CH_2OH$ group is also energetically favorable.

The other mutations did not affect the mode of antagonism. Mutation of hNK$_3$-Y247F$^{5.38}$ did not affect the binding affinity of the two dual NK$_1$/NK$_3$ antagonists **5** and **6**, but mutation of hNK$_3$-H316W$^{6.52}$ affected the binding affinities of both compounds, especially compound **6**. This confirms the binding pose, where compound **6** can get closer to hNK$_3$-His316$^{6.52}$ than compound **5** because of its sulfonamide substituent.

Compounds **3** and **4** were unaffected in their surmountable mode of antagonism by any mutation, which is in agreement with our assumption that both do not form a hydrogen bond with hNK$_3$-Tyr315$^{6.51}$. Binding of compound **3** is affected by hNK$_3$-Y315F$^{6.51}$, although it is more likely due to a change of electronic properties of the aromatic ring and thus its interaction with the basic N in compound **3**. Otherwise, it could be due to a hydrogen bond which would show that the observed effect is specific to this chemical class. As reported previously,[36] compound **3** displayed an insurmountable behavior at the guinea pig NK$_3$ receptor, and the TM2 residue Ala-114$^{2.59}$ in guinea pig NK$_3$ (threonine in all other species) was shown to be involved in this compound's insurmountable behavior by slowing its dissociation kinetics. Interestingly, compound **5** also showed an insurmountable behavior at the guinea pig NK$_3$ receptor,[27] and both mutations hNK$_3$-T139A$^{2.59}$ and gpNK3-A114T$^{2.59}$ had no effect on the insurmountable behavior of compound **5** at human and guinea pig NK$_3$ receptors. Why hNK$_3$-H316W$^{6.52}$ significantly affects the binding of compound **4** cannot be explained by a direct interaction. It is interesting to note that the helix position 6.52 is also a key position for receptor stability, as shown for bovine rhodopsin (Ala269$^{6.52}$),[32] human β2-adrenergic receptor (Phe290$^{6.52}$),[33,34] human A_{2A} adenosine receptor (His250$^{6.52}$),[37] and human dopamine D_3 receptor (Phe346$^{6.52}$).[38]

In agreement with the above hypothesis, the mutation hNK$_1$-F264Y$^{6.51}$ weakened the insurmountable mode of antagonism of compound **5** to a partial insurmountable-like mode of antagonism, resembling the situation in the hNK$_3$ receptor. In this mode of antagonism, an increase of compound **5** concentrations first depressed the maximal response to a limit and then only produced parallel rightward shifts of the SP concentration−response curves. Similar behavior was observed with compounds **7** and **9**. The NK$_1$ selective antagonist compound **1** had previously been shown to have a very slow rate of dissociation from the hNK$_1$ receptor ($t_{1/2}$ of 154 min) and to behave in an insurmountable manner.[19,39] The insurmountable behavior of compound **1** was explained by its slow dissociation rate from the receptor. In the current study, the insurmountable behavior of compound **1** was converted to a surmountable one at mutation hNK$_1$-F264Y$^{6.51}$. This is not surprising because compound **1** also has a hydrogen bond acceptor that can interact with the phenolic OH group. As expected, the mutation hNK$_1$-F264Y$^{6.51}$ had no effect on the surmountable mode of antagonism of compound **2**, another selective NK$_1$ antagonist.[30] Nevertheless, surprisingly, the modes of antagonism of compounds **6**, **8**, **10**, and **11** were not affected by the hNK$_1$-F264Y$^{6.51}$ mutation. A comparison of the ligand binding pockets

dx.doi.org/10.1021/jm2017072 | J. Med. Chem. 2012, 55, 5061−5076

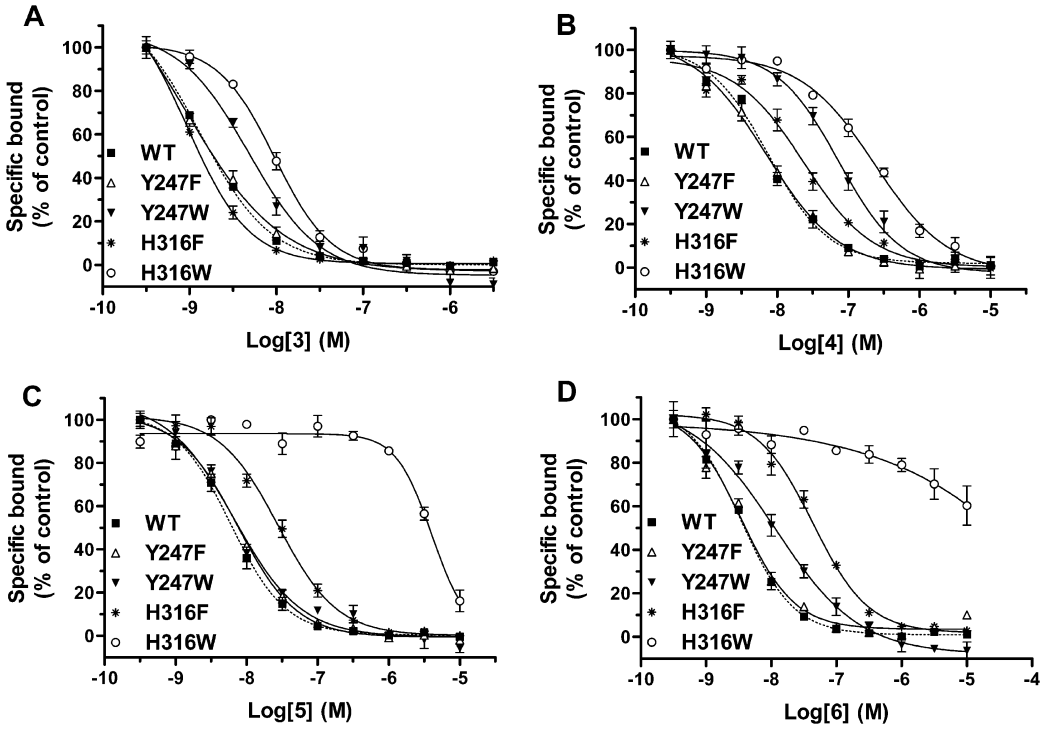

Figure 7. Effects of the mutations at helix positions 5.38 and 6.52 on the competition binding of compounds: **3** (A), **4** (B), **5** (C), and **6** (D) in membrane preparations from HEK293 cells transiently expressing hNK_3-WT, hNK_3-$Y247F^{5.38}$, hNK_3-$Y247W^{5.38}$, hNK_3-$H316F^{6.52}$, or hNK_3-$H316W^{6.52}$. The [^{3}H]**3** at a concentration equal to its K_D value was used in these competition binding experiments. Each data point is the mean ± SE (bars) of three individual experiments performed in duplicate.

of hNK_1 and hNK_3 indicates that there are eight amino acids differences in TM region and ECL2 loop between two receptors, four of them being nonconservative. Therefore, additional factors that are not explained by our model must control the insurmountable mode of antagonism at the hNK_1 receptor of these compounds.

Finally, a high resolution X-ray structure of hβ2AR has revealed that four residues $Trp286^{6.48}$ (key residue of the rotamer toggle switch), $Phe289^{6.51}$, $Phe290^{6.52}$ in TM6 and $Phe208^{5.47}$ in TM5 are involved in the toggle switch mechanism of β2AR activation.[33,34] A rotameric change of $Trp286^{6.48}$ is thought to occur in the activation step, and the residue at helix position 6.51 (Phe289), as part of a ring face aromatic interaction, can stabilize the active conformation. It is also interesting to note that recent findings have demonstrated that four out of nine multiplex families affected by hypogonadotropic hypogonadism carry loss-of-function mutations in NKB or the hNK_3 receptor, indicating that this system also plays a key role in the central neuroendocrine control of reproduction in humans.[40] Remarkably, the homozygous loss-of-function mutation hNK_3-Y315C found in these patients with reproductive dysfunction[41] is located at the helix position 6.51, which corresponds to the residue hNK_3-$Tyr315^{6.51}$ (or hNK_1-$Phe264^{6.51}$) that we have found to contribute to an insurmountable mode of antagonism of NK_1/NK_3 antagonists. Taken together, hNK_3-$Tyr315^{6.51}$ (or hNK_1-$Phe264^{6.51}$) occupies a critical position in the TM6, which is involved in receptor stability and activation.

In conclusion, we have shown in molecular details the likely mechanism of the insurmountable behavior of the dual NK_1/NK_3 antagonist **5** and a few structural analogues. Interestingly, this insurmountable mode of antagonism observed in vitro translates to a long-lasting in vivo receptor blockade by compound **5** (half-life $t_{1/2}$ = 14 h).[27] As it has already been well documented for the angiotensin AT1 receptor and many other GPCRs,[42−46] the ability of antagonists to form slowly dissociating complexes with their cognate receptors is being proposed to be responsible for their long-lasting clinical actions. It remains to be determined whether the residue at helix position 6.51 has a similar key contribution to the insurmountable behavior of other antagonists in interactions with their cognate peptide GPCRs. This would be of high importance because it might further assist the development of drugs with an insurmountable mode of antagonism and a long duration of in vivo action.

EXPERIMENTAL SECTION

Chemistry. General. Solvents and reagents of commercial quality were used as purchased. Column chromatography was carried out on silica gel 60 (32−60 mesh, 60 Å) or on prepacked columns (Isolute Flash Si). ^{1}H NMR spectra were recorded on a Bruker AvanceIII 600 cryo-TCI spectrometer with the residual solvent peak as the internal reference (i.e., $CDCl_3$ = 7.26 ppm). ^{1}H resonances are reported to the nearest 0.01 ppm. The multiplicities of signals are given as s = singlet, d = doublet, t = triplet, q = quartet, br = broad, and combinations thereof. Coupling constants (J) are reported to the nearest 0.01 Hz. High resolution mass spectrometry (HRMS) was performed on a Agilent 6520 spectrometer using time-of-flight (TOF) with positive ESI or EI at 70 eV within a tolerance of ±5 ppm of the theoretical value. The purity of compounds **5**−**11** was determined as >95% by HPLC analysis. Parameters were as follows: system, Agilent 1290 LC with CTC PAL coupled to a Agilent 6520 QTOF; column, Zorbax Eclipse Plus C18 2.1 mm × 50 mm, 1.8 μm (Agilent purchase no. 959757-902); eluent A, 1 L of H_2O + 0.2 mL of HCOOH; eluent B, 80% ACN, 20% 3i-PrOH, 0.01% HCOOH; initial, 5% B; column temperature, 55 °C; detection wavelength, 220 ± 5 nm.

dx.doi.org/10.1021/jm2017072 | J. Med. Chem. 2012, 55, 5061−5076

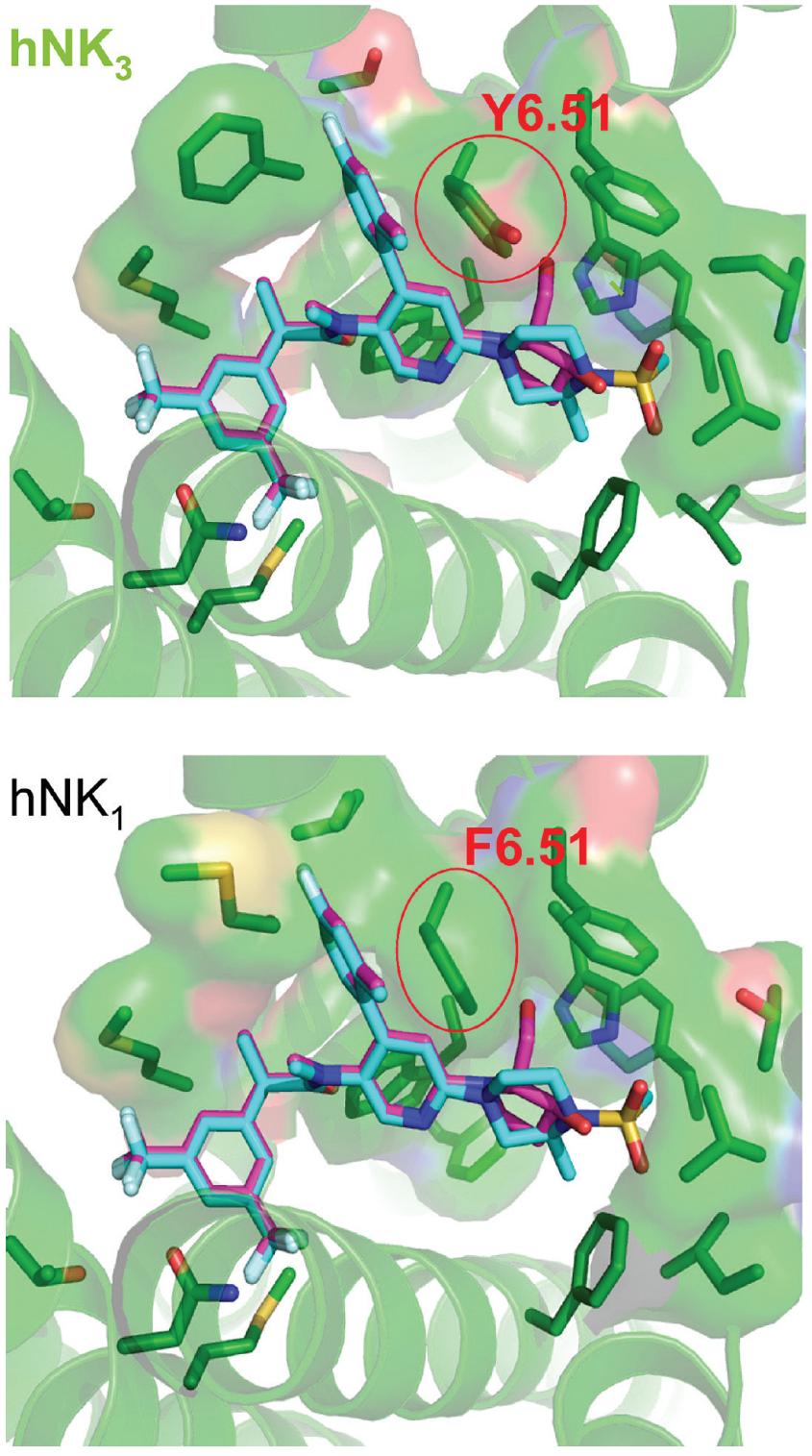

Figure 8. Compounds **5** (magenta) and **6** (cyan) docked into the homology model of the human NK_3 receptor (top) and human NK_1 receptor (bottom). Carbon atoms of the protein are shown in green.

Reference Compounds 1−4. 2-(*R*)-(1-(*R*)-3,5-Bis(trifluoromethyl)phenylethoxy)-3-(*S*)-(4-fluoro)phenyl-4-(3-oxo-1,2,4-triazol-5yl)methylmorphine) (**1**, aprepitant, MK-869),[19] (2*S*,3*S*)-*cis*-2-(diphenylmethyl)-*N*-[(2-methoxyphenyl)methyl]-1-azabicyclo[2.2.2]octan-3-amine (**2**, CP-96,345),[30] (*S*)-(+)-*N*-((3-[1-benzoyl-3-(3,4-dichlorophenyl)piperidin-3-yl]prop-1-yl)-4-phenylpiperidin-4-yl)-*N*-methylacetamine (**3**, osanetant, SR 142801),[3,4] (*S*)-(−)-*N*-(α-ethylbenzyl)-3-hydroxy-2-phenylquinoline-4-carboxamide (**4**, talnetant, SB 223412),[5,6] and (*S*)-(−)-*N*-(α-ethylbenzyl)-3-methyl-2-phenylquinoline-4-carboxamide (SB 222200)[5] were synthesized according to procedures described in the literature, and their purity was confirmed (>95% by HPLC analysis).

Synthesis. (2*R*,3*S*)-2-(3,5-Bis-trifluoromethylphenyl)-*N*-[4-(4-fluoro-2-methylphenyl)-6-(3-hydroxy-2-hydroxymethylpyrrolidin-1-yl)pyridin-3-yl]-*N*-methylisobutyramide (5, RO4583298).[25] A mixture of 11.0 g (20.6 mmol) of 2-(3,5-bis-trifluoromethyl-phenyl)-*N*-[6-chloro-4-(4-fluoro-2-methylphenyl)pyridin-3-yl]-*N*-methylisobutyramide,[25] 14.3 g (103 mmol) of potassium carbonate, and 12.2 g

dx.doi.org/10.1021/jm2017072 | *J. Med. Chem.* 2012, 55, 5061−5076

(75.7 mmol) of (2*R*,3*S*)-2-(hydroxymethyl)-3-hydroxypyrrolidine in 110 mL dimethyl sulfoxide was stirred at 130 °C for 68 h. The reaction mixture was diluted with 800 mL of ethyl acetate and washed with 800 mL of saturated sodium carbonate solution, 500 mL of water, and 750 mL of brine. The combined aqueous layers were extracted with two 800 mL portions of ethyl acetate. The combined organic layers were dried over sodium sulfate and concentrated in vacuo. Purification by flash chromatography gave 8.48 g (67%) of **5** as off-white foamy solid. ^{1}H NMR (600 MHz, $CDCl_3$) δ 7.86 (d, J = 11.69 Hz, 1H), 7.76 (s, 1H), 7.63 (br s, 2H), 7.19−7.34 (m, 1H), 6.95 (br s, 2H), 6.31 (br s, 1H), 5.29−6.10 (m, 1H), 4.13−4.47 (m, 2H), 3.79−3.96 (m, 1H), 3.37−3.73 (m, 3H), 1.90−2.69 (m, 8H), 1.07−1.73 (m, 6H); HRMS calcd for $C_{30}H_{30}F_7N_3O_3$, 613.2175; found, 613.218.

(*S*)-2-(3,5-Bis-trifluoromethylphenyl)-*N*-[4-(4-fluoro-2-methylphenyl)-6-((*S*)-4-methanesulfonyl-3-methylpiperazin-1-yl)-pyridin-3-yl]-*N*-methylisobutyramide (6, RO4908594).[25] (a) A mixture of 0.20 g (0.38 mmol) of 2-(3,5-bis-trifluoromethylphenyl)-*N*-[6-chloro-4-(4-fluoro-2-methylphenyl)pyridin-3-yl]-*N*-methylisobutyramide,[25] 0.11 g (1.1 mmol) of (*S*)-2-methylpiperazine, and 0.10 g (0.72 mmol) of potassium carbonate in 0.3 mL of dimethyl sulfoxide was heated at 180 °C under microwave irradiation in a sealed tube for 30 min. After cooling to room temperature, the reaction mixture was diluted with a 0.3 M aqueous solution of sodium hydroxide and extracted with three portions of *tert*-butyl methyl ether. The combined organic extracts were dried over sodium sulfate and concentrated. Purification by silica gel column chromatography gave 0.12 g (51%) of (*S*)-2-(3,5-bis-trifluoromethylphenyl)-*N*-[4-(4-fluoro-2-methylphenyl)-6-(3-methylpiperazin-1-yl)pyridin-3-y1]-*N*-methylisobutyramide as an off-white solid. MS *m*/*e* (%): 597 (M + H$^+$, 100). (b) To a solution of 0.19 g (0.31 mmol) of (*S*)-2-(3,5-bistrifluoromethylphenyl)-*N*-[4-(4-fluoro-2-methylphenyl)-6-(3-methylpiperazin-l-yl)pyridin-3-yl]-*N*-methylisobutyramide and 38 mg (0.38 mmol) of triethylamine in 4 mL of dichloromethane was added 38 mg (0.33 mmol) of methanesulfonyl chloride at 0 °C. After the addition was completed, the reaction mixture was allowed to warm to room temperature. Conversion was monitored by thin layer chromatography. After complete consumption of the starting material the reaction mixture was diluted with water and extracted with three portions of *tert*-butyl methyl ether. The combined organic layers were dried over sodium sulfate and concentrated in vacuo. Purification by silica gel column chromatography gave 0.15 g (75%) of **6** as a white solid. ^{1}H NMR (600 MHz, $CDCl_3$) δ 7.98 (s, 1H), 7.77 (s, 1H), 7.56−7.70 (m, 2H), 7.22−7.25 (m, 1H), 6.95 (br s, 2H), 6.44 (s, 1H), 4.16−4.35 (m, 2H), 3.96−4.15 (m, 1H), 3.67 (d, J = 12.79 Hz, 1H), 3.34 (t, J = 11.23 Hz, 1H), 3.26 (d, J = 10.48 Hz, 1H), 2.99−3.13 (m, 1H), 2.90 (s, 3H), 2.58 (br s, 1H), 2.35 (br s, 2H), 2.26 (br s, 1H), 2.11 (br s, 2H), 1.45−1.60 (m, 3H), 1.28−1.45 (m, 6H); HRMS calcd for $C_{31}H_{33}F_7N_4O_3S$, 674.2162; found, 674.2179.

(2*S*)-2-(3,5-Bis-trifluoromethylphenyl)-*N*-[4-(4-fluoro-2-methylphenyl)-6-(2-hydroxymethylpyrrolidin-1-yl)pyridin-3-yl]-*N*-methylisobutyramide (Compound 7, RO4603325).[25] A mixture of 0.20 g (0.38 mmol) of 2-(3,5-bis-trifluoromethylphenyl)-*N*-[6-chloro-4-(4-fluoro-2-methylphenyl)pyridin-3-yl]-*N*-methylisobutyramide,[25] 0.23 g (2.3 mmol) of L-prolinol, and 0.15 g (1.1 mmol) of potassium carbonate in 0.5 mL of dimethyl sulfoxide was heated at 180 °C under microwave irradiation for 30 min in a sealed tube. After cooling to room temperature, the reaction mixture was diluted with water and extracted with three portions of *tert*-butyl methyl ether. The combined organic extracts were washed with water and brine, dried over sodium sulfate, and concentrated in vacuo. Purification by silica gel column chromatography gave 0.18 g (78%) of **7** as off-white solid. ^{1}H NMR (600 MHz, $CDCl_3$) δ 7.81−7.96 (m, 1H), 7.76 (s, 1H), 7.63 (br s, 2H), 7.19−7.35 (m, 1H), 6.77−7.05 (m, 2H), 6.25 (s, 2H), 4.24−4.47 (m, 1H), 3.55−3.86 (m, 2H), 3.14−3.51 (m, 2H), 1.88−2.74 (m, 9H), 1.74 (br s, 1H), 1.15−1.66 (m, 6H); HRMS calcd for $C_{30}H_{30}F_7N_3O_2$, 597.2226; found, 597.222.

(*S*)-2-(3,5-Bis-trifluoromethylphenyl)-*N*-[4-(4-fluoro-2-methylphenyl)-6-(3-hydroxypyrrolidin-1-yl)pyridin-3-yl]-*N*-methylisobutyramide (Compound 8, RO4746092).[25] Off-white foamy solid after purification by silica gel column chromatography. ^{1}H NMR (600 MHz, $CDCl_3$) δ 7.96 (s, 1H), 7.76 (s, 1H), 7.65 (br s, 2H), 7.21−7.31 (m, 1H), 6.94 (br s, 2H), 6.19 (s, 1H), 4.62 (br s, 1H), 3.45−3.71 (m, 4H), 2.04−2.68 (m, 8H), 1.17−1.86 (m, 6H); HRMS calcd for $C_{29}H_{28}F_7N_3O_2$, 583.207; found, 583.2075.

(*S*)-2-(3,5-Bis-trifluoromethylphenyl)-*N*-[4-(4-fluoro-2-methylphenyl)-6-(2-hydroxymethyl-4-methanesulfonylpiperazin-1-yl)wpyridin-3-yl]-*N*-methylisobutyramide (Compound 9, RO4861497).[25] Off-white solid after purification by silica gel column chromatography. ^{1}H NMR (600 MHz, $CDCl_3$) δ 7.96 (br s, 1H), 7.77 (s, 1H), 7.64 (br s, 2H), 7.18−7.32 (m, 1H), 6.96 (br s, 2H), 6.52 (br s, 1H), 4.42−4.77 (m, 1H), 4.11−4.16 (m, 1H), 4.25 (br s, 1H), 3.91−4.01 (m, 2H), 3.81 (d, J = 11.48 Hz, 2H), 3.18−3.43 (m, 1H), 2.98 (dd, J = 3.63, 12.09 Hz, 1H), 2.88−2.95 (m, 1H), 2.77−2.87 (m, 3H), 1.98−2.72 (m, 6H), 1.18−1.71 (m, 6H); HRMS calcd for $C_{31}H_{33}F_7N_4O_4S$, 690.2111; found, 690.211.

2-(3,5-Bis-trifluoromethylphenyl)-*N*-[4-(4-fluoro-2-methylphenyl)-6-(4-methanesulfonylpiperazin-1-yl)pyridin-3-yl]-*N*-methylisobutyramide (Compound 10, RO4858154).[25] White solid after purification by silica gel column chromatography. ^{1}H NMR (600 MHz, $CDCl_3$) δ 8.01 (s, 1H), 7.77 (s, 1H), 7.65 (br s, 2H), 7.18−7.32 (m, 1H), 6.96 (br s, 2H), 6.50 (s, 1H), 3.54−3.85 (m, 4H), 3.33 (t, J = 5.04 Hz, 4H), 2.81 (s, 3H), 2.01−2.65 (m, 6H), 1.17−1.67 (m, 6H); HRMS calcd for $C_{30}H_{31}F_7N_4O_3S$, 660.2005; found, 660.201.

2-(3,5-Bis-trifluoromethylphenyl)-*N*-[6-(4,4-dioxo-1-oxa-4λ^6-thia-8-aza-spiro[4.5]dec-8-yl)-4-(4-fluoro-2-methylphenyl)-pyridin-3-yl]-*N*-methylisobutyramide (Compound 11, RO4896062).[25] White solid after purification by silica gel column chromatography. ^{1}H NMR (600 MHz, $CDCl_3$) δ 7.99 (s, 1H), 7.77 (s, 1H), 7.65 (br s, 2H), 7.19−7.33 (m, 1H), 6.78−7.06 (m, 2H), 6.51 (s, 1H), 4.34 (t, J = 6.90 Hz, 2H), 4.16 (br s, 1H), 4.01 (br s, 1H), 3.48 (br s, 2H), 3.25 (t, J = 6.90 Hz, 2H), 2.59 (br s, 1H), 2.35 (br s, 2H), 2.27 (br s, 1H), 2.12 (br s, 4H), 1.94 (d, J = 13.30 Hz, 2H), 1.46−1.61 (m, 3H), 1.31−1.44 (m, 3H); HRMS calcd for $C_{32}H_{32}F_7N_3O_4S$, 687.2002; found, 687.2002.

Materials. Radioligands [^{3}H]**3** ([^{3}H]SR 142801) (catalog no. TRK1035, specific activity of 74.0 Ci/mmol, radiochemical purity of 99.7% by HPLC, Novapak C18 column) and [^{3}H]SP ([^{3}H]substance P, catalog no. TRK786, specific activity of 40.0 Ci/mmol) were purchased from GE Healthcare UK Ltd., Chalfont St. Giles, U.K. [MePhe^7]-Neurokinin B (Asp-Met-His-Asp-Phe-Phe-NMe-Phe-Gly-Leu-Met-NH_2, catalog no. SC981) was purchased from NeoMPS SA (Strasbourg, France). Substance P (Arg-Pro-Lys-Pro-Gln-Gln-Phe-Phe-Gly-Leu-Met-NH_2, catalog no. 1156) was obtained from Tocris Biosciences (Bristol, U.K.). [*myo*-1,2-^{3}H]Inositol with PT6-271 (TRK911, specific activity of 16.0 Ci/mmol) and yttrium silicate (Ysi) RNA binding SPA beads (RPNQ0013) were purchased from GE Healthcare.

Plasmids, Cell Culture, and Membrane Preparation. The cDNAs encoding human NK_1 receptor (accession number P25103) and human NK_3 receptor (accession number P29371) were subcloned into pCI-Neo expression vectors (Promega Corporation, Madison, WI). All point mutants were constructed using the QuickChange site-directed mutagenesis kit (catalog no. 200518, Stratagene, La Jolla, CA).The entire coding regions of all point mutants were sequenced from both strands using an automated cycle sequencer (Applied Biosystems, Foster City, CA).

Human embryonic kidney (HEK)293 cells were transfected as previously described.[31] Forty-eight hours posttransfection, the cells were harvested and washed three times with ice-cold PBS and frozen at −80 °C. The pellet was suspended in ice-cold 50 mM Tris-HCl pH 7.4 buffer containing 10 mM EDTA (10× volume) and homogenized with a Polytron (Kinematica AG, Basel, Switzerland) for 30 s at 16 000 rpm After centrifugation at 48000*g* for 30 min at 4 °C, the pellet was suspended again in ice-cold 10 mM Tris pH 7.4 buffer containing 0.1 mM EDTA (10× volume), homogenized, and spun again as above. The pellet was resuspended in ice-cold 10 mM Tris pH 7.4 buffer containing 0.1 mM EDTA and 10% sucrose (5× volume). The membrane homogenate was frozen at −80 °C before use.

Radioligand Binding. After thawing, the membrane homogenates were centrifuged at 48000*g* for 10 min at 4 °C. The pellets were resuspended in the binding buffer. The assay buffers consisted of the following: for NK_1, 50 mM Hepes, 3 mM $MnCl_2$, 2 μM phosphoramidon, 16.8 μM Leupeptin, 0.04% BSA binding buffer at pH 7.4; for NK_3, 50 mM Tris-HCl, 4 mM $MnCl_2$, 1 μM phosphoramidon, 0.1% bovine serum albumin at pH 7.4. Final assay

dx.doi.org/10.1021/jm2017072 | J. Med. Chem. 2012, 55, 5061−5076

concentration for hNK_1-WT and hNK_1-F264Y expressing membranes was 2.5 μg protein/well, and for hNK_3-WT and hNK_3-Y315F expressing membranes it was 5 μg protein/well. Saturation isotherms were determined by addition of various concentrations of radioligand [^{3}H]SP (NK_1, 0.04−18 nM) or [^{3}H]**3** (NK_3, 0.009−3 nM) to membranes (in a total reaction volume of 500 μL) for 90 min, respectively, at room temperature (rt). Nonspecific binding was determined with 10 μM compound **2** (NK_1) and 10 μM SB 222200 (NK_3). At the end of the incubation, membranes were filtered onto 96-well white microplates (preincubated for 1 h in 0.3% polyethylenimine + 0.1% bovine serum albumin) with a bonded GF/C filter for [^{3}H]SP and [^{3}H]**3** binding (PerkinElmer Life and Analytical Sciences, Waltham, MA), with a FilterMate-96 well harvester (PerkinElmer Life and Analytical Sciences), and washed 4 times with ice-cold 50 mM Tris-HCl, pH 7.4 buffer. The radioactivity on the filter was counted (5 min) on a Packard Top-Count microplate scintillation counter with quenching correction after addition of 45 μL of microscint 40 (Canberra Packard S.A., Zürich, Switzerland) and 1 h of agitation. Saturation experiments were analyzed by Prism 5.0 (GraphPad software, San Diego, CA) using the rectangular hyperbolic equation derived from the equation of a bimolecular reaction and the law of mass action, $B = (B_{max}[F])/(K_D + [F])$, where B is the amount of ligand bound at equilibrium, B_{max} (the maximum number of binding sites) is the specific binding extrapolated to very high concentrations of radioligand, [F] is the concentration of free ligand, and K_D (the ligand dissociation constant) is the radioligand concentration needed to achieve a half-maximum binding at equilibrium. For inhibition experiments, membranes were incubated with radioligand at a concentration equal to K_D of the radioligand and 10 concentrations of the competing compound (0.0003−10 μM). The IC_{50} values (inhibition concentration at which 50% specific binding of the radioligand was displaced) were derived from the inhibition curve using a sigmoidal dose−response (variable slope), which is also known as a four-parameter/nonlinear regression analysis (GraphPad Prism 5) as shown in the equation $Y = Y_{min} + (Y_{max} - Y_{min})/(1 + 10^{((\log IC_{50} - X)n_H)})$, where Y is the % specific binding, Y_{min} is the minimum Y, Y_{max} is the maximum Y, X is the concentration of the competing compound, and n_H is the slope of the curve (the Hill coefficient). The affinity constant (K_i) values were calculated using the Cheng−Prussoff equation $K_i = IC_{50}/(1 + [L]/K_D)$ where [L] is the concentration of radioligand and K_D is its dissociation constant at the receptor, derived from the saturation isotherm. Statistical significance was determined using a two-tailed unpaired Student's t test (Prism 5.0, GraphPad software).

[^{3}H]Inositol Phosphate (IP) Accumulation Assay. [^{3}H]IP accumulation was measured as described previously with the following adaptations.[36] HEK293 cells were transfected with various NK cDNAs in pCl-Neo using Lipofectamine Plus reagent (Invitrogen) according to the manufacturer's instructions. After 24 h posttransfection, cells were washed twice in labeling medium: Dulbecco's modified Eagle's medium without inositol (MP Biomedicals, Irvine, CA), 10% fetal calf serum, 1% penicillin/streptomycin, and 2 mM glutamate. Cells were seeded at 8×10^4 cells/well in poly-D-lysine-treated 96-well plates in the labeling medium supplemented with 5 μCi/mL *myo*-[1,2-^{3}H]-inositol. On the day of assay (48 h posttransfection), cells were washed three times with the buffer (1× HBSS, 20 mM HEPES, pH 7.4) and then incubated for 10 min at rt in assay buffer (1× HBSS, 20 mM HEPES, pH 7.4, plus 8 mM LiCl to prevent phosphotidylinositide breakdown) prior to the addition of agonists or antagonists. Antagonists were incubated for 20 min at 37 °C prior to stimulation with the agonist, either SP (NK_1) or [MePhe^7]NKB (NK_3), at concentrations ranging from 1 μM to 0.01 nM. For surmountable or insurmountable antagonism assessment, Schild analyses were performed. The agonist curves were generated in the presence of increasing concentrations of antagonist, and the shift in agonist EC_{50} or depression in maximum response was determined. After 45 min of incubation at 37 °C with the agonist, the assay was terminated by the aspiration of the assay buffer and the addition of 100 μL of 20 mM formic acid to lyse the cells. After shaking for 30 min at 23 °C, a 40 μL aliquot was mixed with 80 μL of yttrium silicate RNA binding SPA beads (12.5 mg/mL, bind the inositol phosphates but not the inositol) and then shaken for 30 min at 23 °C. Assay plates were centrifuged for 2 min at 750g prior to counting on a Packard Top-Count microplate scintillation counter with quenching correction (PerkinElmer Life and Analytical Sciences). For PI hydrolysis, activation and inhibition curves were fitted according to the equation $y = A + (B - A)/[1 + (C/x)^D]$, where A is y_{min}, B is y_{max}, C is EC_{50}, and D is the Hill slope factor, using ExcelFit 3.0 (IDBS software). The relative efficacy (E_{max}) values of SP or [MePhe^7]NKB was calculated as the fitted maximum of the concentration−response curve of each mutated receptor expressed as a percentage of fitted maximum of the wild type (WT) concentration−response curve from cells transfected and assayed on the same day.

Residue Numbering Scheme. The position of each amino acid residue in the 7TMD is identified both by its sequence number and by its generic numbering system proposed by Ballesteros and Weinstein[47] which is shown as superscript. In this numbering system, amino acid residues in the 7TMD are given two numbers. The first refers to the TM number, and the second indicates its position relative to a highly conserved residue of class A GPCRs in that TM, which is arbitrarily assigned 50. The amino acids in the extracellular loop ECL2 are labeled 45 to indicate their location between the helixes 4 and 5. The highly conserved cysteine thought to be disulfide bonded was given the index number 45.50 (SWISS-PROT: opsd_bovin C187), and the residues within the ECL2 loop are then indexed relative to the "50" position.

Model Building. The amino acid sequences of the human NK_3 (accession number P29371), rat NK_3 (accession number P16177), mouse NK_3 (accession number P47937), gerbil NK_3 (accession number AM157740), human NK_1 (accession number P25103), and human NK_2 (accession number P21452) were retrieved form the Swiss-Prot database. These amino acid sequences were aligned to the sequence of bovine rhodopsin (accession number P02699) using the ClustalW multiple alignment program. A slow pairwise alignment using the BLOSUM matrix series[48] and a gap opening penalty of 15.0 were chosen for aligning the amino acid sequences. Other parameters were those given as default. The sequences were aligned in two steps: (i) from the N-terminus to the first five residues of the third intracellular loop (ICL3) and (ii) from the last five residues of the ICL3 loop to the C-terminus. The ICL3 loop was excluded from the alignment, since it shows too high variability in amino acid composition and length. The alignments were then verified to ensure that conserved residues of the transmembrane regions were aligned and manually adjusted in the second extracellular loop (ECL2) in order to align the conserved cysteine which takes part in the disulfide bridges occurring between the third transmembrane segment (TM3) and the second extracellular loop (ECL2).

By use of this alignment and the X-ray structure of bovine rhodopsin[32] as template, the software package MOE (MOE, version 2005.05, Chemical Computing Group, Montreal, Quebec, Canada) was used to generate a three-dimensional model of the hNK_3. Ten intermediate models were generated, and the best one was selected as the final MOE model. No minimization was used in order to keep the backbone coordinates as in the X-ray structure. After the heavy atoms were modeled, all hydrogen atoms were added in appropriate locations with the preparatory program PROTONATE of AMBER, version 6 (University of California, San Francisco). Compound **3** was then manually docked into the transmembrane cavity of the hNK_3 model. The docking mode was based on the following hypotheses: (1) The ligand should make a direct interaction with Met134$^{2.53}$, since this residue has been shown to be responsible for species selectivity of *N*-[(*S*)-4-(4-acetylamino-4-phenylpiperidin-1-yl)-2-(3,4-dichlorophenyl)-butyl]-*N*-methylbenzamide (saredutant, SR 48968).[49] (2) Phenylpiperidine substructures are privileged fragments for the subpocket formed by the transmembrane domains 3, 5, and 6. The resulting protein−ligand complex was then minimized using AMBER, version 6. The minimization was carried out using 5000 steps of steepest descent followed by conjugate gradient minimization until the rms (root-mean-square) gradient of the potential energy was less than 0.05 kcal mol^{-1} Å^{-1}. A twin cutoff (10.0, 15.0 Å) was used to calculate nonbonded electrostatic interactions at every minimization step and the nonbonded pair list was update every 25 steps. A distance-dependent

($\varepsilon = 4r$) dielectric function was used. Removing the ligand from the complex yielded the final coordinates of the hNK_3 model. (*S*)-(−)-*N*-(α-Ethylbenzyl)-3-methoxy-2-phenylquinoline-4-carboxamide (Me-talnetant, analogue of compound **4**)[31] was then manually docked into the receptor. The proposed docking mode is based on the SAR (structure−activity relationships) of compound **4** according to which at position 3 similar side chains as used in the compound **3** series can be added. The 3-methoxy group of Me-talnetant has thus to point into the direction of the subpocket TM3, -5, and -6. We additionally docked compound **6**.[31] This compound was previously aligned onto compound **3** by comparison of the observed SAR of the compound **3** series[50] and the compound **6** chemical series.[25] Thus, its docking mode was guided by the docking pose of compound **3** and this ligand alignment. The resulting docking poses have been used for site-directed mutagenesis studies. The results of these studies were in agreement with our proposed docking poses and have been published previously.[31] However, we state clearly that this is not at all proof that the docking hypotheses represent the true binding mode.

The described docking mode of the NK_1/NK_3 antagonist **6** was used to align and dock the close analogue compound **5** and further derivatives of this chemical series used in the present study. We have also reconstructed a hNK_3 model based on the human β2-adrenergic receptor crystal structure (PDB code 2RH1),[33,34] but this model did not fit the NK_3 antagonists as well as the model based on rhodopsin. It relates to the fact that TM2 and especially TM5 are moved further inside the transmembrane cavity in hβ2AR than in the rhodopsin structure, thus limiting the space. The hNK_3 model was used to build a homology model of the hNK_1 using MOE based on the alignment described previously.[31] The NK_1 antagonists **1** and **2** were docked into the model in analogy to the NK_1/NK_3 antagonists.

AUTHOR INFORMATION

Corresponding Author

*Phone: +41-61-4612858. E-mail: parichehr.malherbe@roche.com.

Notes

The authors declare no competing financial interest.

ACKNOWLEDGMENTS

We thank Janine Holger and Marie-Thérèse Zenner for their excellent technical assistance; Cosimo Dolente, Andreas Koblet, Beat Bucher, and Julien Heusser for the skilled synthesis of compounds **5**−**11**; and Dr. Josef Schneider for analytical assistance. We are grateful to Dr. Andrew Thomas for his critical reading of the manuscript.

ABBREVIATIONS USED

SP, substance P; NK, neurokinin; NKA, neurokinin A; NKB, neurokinin B; NK_1, neurokinin 1 receptor; NK_2, neurokinin 2 receptor; NK_3, neurokinin 3 receptor; GPCR, G-protein-coupled receptor; IP, inositol phosphate; DAG, diacylglycerol; 7TMD, seven-transmembrane domain; 5-HT, 5-hydroxytryptamine; $5\text{-}HT_{2A}$, 5-hydroxytryptamine type 2A receptor; D_2, dopamine type 2 receptor; WT, wild type; HEK, human embryonic kidney; OPSD, bovine rhodopsin; β_2AR, β2-adrenergic receptor

REFERENCES

(1) Tamminga, C. A.; Holcomb, H. H. Phenotype of schizophrenia: a review and formulation. *Mol. Psychiatry.* **2005**, *10*, 27−39.

(2) Leucht, S.; Wahlbeck, K.; Hamann, J.; Kissling, W. New generation antipsychotics versus low-potency conventional antipsychotics: a systematic review and meta-analysis. *Lancet* **2003**, *361*, 1581−1589.

(3) Emonds-Alt, X.; Bichon, D.; Ducoux, J. P.; Heaulme, M.; Miloux, B.; Poncelet, M.; Proietto, V.; Van Broeck, D.; Vilain, P.; Neliat, G.; et al. SR 142801, the first potent non-peptide antagonist of the tachykinin NK3 receptor. *Life Sci.* **1995**, *56*, PL27−PL32.

(4) Nguyen-Le, X. K.; Nguyen, Q. T.; Gobeil, F.; Pheng, L. H.; Emonds-Alt, X.; Breliere, J. C.; Regoli, D. Pharmacological characterization of SR 142801: a new non-peptide antagonist of the neurokinin NK-3 receptor. *Pharmacology* **1996**, *52*, 283−291.

(5) Giardina, G. A.; Raveglia, L. F.; Grugni, M.; Sarau, H. M.; Farina, C.; Medhurst, A. D.; Graziani, D.; Schmidt, D. B.; Rigolio, R.; Luttmann, M.; Cavagnera, S.; Foley, J. J.; Vecchietti, V.; Hay, D. W. Discovery of a novel class of selective non-peptide antagonists for the human neurokinin-3 receptor. 2. Identification of (*S*)-*N*-(1-phenylpropyl)-3-hydroxy-2-phenylquinoline-4-carboxamide (SB 223412). *J. Med. Chem.* **1999**, *42*, 1053−1065.

(6) Sarau, H. M.; Griswold, D. E.; Potts, W.; Foley, J. J.; Schmidt, D. B.; Webb, E. F.; Martin, L. D.; Brawner, M. E.; Elshourbagy, N. A.; Medhurst, A. D.; Giardina, G. A.; Hay, D. W. Nonpeptide tachykinin receptor antagonists: I. Pharmacological and pharmacokinetic characterization of SB 223412, a novel, potent and selective neurokinin-3 receptor antagonist. *J. Pharmacol. Exp. Ther.* **1997**, *281*, 1303−1311.

(7) Meltzer, H.; Prus, A. NK3 receptor antagonists for the treatment of schizophrenia. *Drug Discovery Today: Ther. Strategies* **2006**, *3*, 555−560.

(8) Meltzer, H. Y.; Arvanitis, L.; Bauer, D.; Rein, W. Placebo-controlled evaluation of four novel compounds for the treatment of schizophrenia and schizoaffective disorder. *Am. J. Psychiatry* **2004**, *161*, 975−984.

(9) Spooren, W.; Riemer, C.; Meltzer, H. Opinion: NK3 receptor antagonists: the next generation of antipsychotics? *Nat. Rev. Drug Discovery* **2005**, *4*, 967−975.

(10) Dawson, L. A.; Smith, P. W. Therapeutic utility of NK3 receptor antagonists for the treatment of schizophrenia. *Curr. Pharm. Des.* **2010**, *16*, 344−357.

(11) Alexander, S. P.; Mathie, A.; Peters, J. A. Guide to receptors and channels (GRAC), 5th edition. *Br. J. Pharmacol.* **2011**, *164* (Suppl. 1), S1−S324.

(12) Almeida, T. A.; Rojo, J.; Nieto, P. M.; Pinto, F. M.; Hernandez, M.; Martin, J. D.; Candenas, M. L. Tachykinins and tachykinin receptors: structure and activity relationships. *Curr. Med. Chem.* **2004**, *11*, 2045−2081.

(13) Severini, C.; Improta, G.; Falconieri-Erspamer, G.; Salvadori, S.; Erspamer, V. The tachykinin peptide family. *Pharmacol. Rev.* **2002**, *54*, 285−322.

(14) Marco, N.; Thirion, A.; Mons, G.; Bougault, I.; Le Fur, G.; Soubrie, P.; Steinberg, R. Activation of dopaminergic and cholinergic neurotransmission by tachykinin NK3 receptor stimulation: an in vivo microdialysis approach in guinea pig. *Neuropeptides* **1998**, *32*, 481−488.

(15) Dawson, L. A.; Cato, K. J.; Scott, C.; Watson, J. M.; Wood, M. D.; Foxton, R.; de la Flor, R.; Jones, G. A.; Kew, J. N.; Cluderay, J. E.; Southam, E.; Murkitt, G. S.; Gartlon, J.; Pemberton, D. J.; Jones, D. N.; Davies, C. H.; Hagan, J. In vitro and in vivo characterization of the non-peptide NK3 receptor antagonist SB-223412 (talnetant): potential therapeutic utility in the treatment of schizophrenia. *Neuropsychopharmacology* **2008**, *33*, 1642−1652.

(16) Ebner, K.; Muigg, P.; Singewald, G.; Singewald, N. Substance P in stress and anxiety: NK-1 receptor antagonism interacts with key brain areas of the stress circuitry. *Ann. N.Y. Acad. Sci.* **2008**, *1144*, 61−73.

(17) Blier, P.; Gobbi, G.; Haddjeri, N.; Santarelli, L.; Mathew, G.; Hen, R. Impact of substance P receptor antagonism on the serotonin and norepinephrine systems: relevance to the antidepressant/anxiolytic response. *J. Psychiatry Neurosci.* **2004**, *29*, 208−218.

(18) Santarelli, L.; Gobbi, G.; Debs, P. C.; Sibille, E. T.; Blier, P.; Hen, R.; Heath, M. J. Genetic and pharmacological disruption of neurokinin 1 receptor function decreases anxiety-related behaviors and increases serotonergic function. *Proc. Natl. Acad. Sci. U.S.A.* **2001**, *98*, 1912−1917.

(19) Hale, J. J.; Mills, S. G.; MacCoss, M.; Finke, P. E.; Cascieri, M. A.; Sadowski, S.; Ber, E.; Chicchi, G. G.; Kurtz, M.; Metzger, J.; Eiermann, G.; Tsou, N. N.; Tattersall, F. D.; Rupniak, N. M.; Williams, A. R.; Rycroft, W.; Hargreaves, R.; MacIntyre, D. E. Structural optimization affording 2-(*R*)-(1-(*R*)-3, 5-bis(trifluoromethyl)-phenylethoxy)-3-(*S*)-(4-fluoro)phenyl-4-(3-oxo-1,2,4-triazol-5-yl)-methylmorpholine, a potent, orally active, long-acting morpholine acetal human NK-1 receptor antagonist. *J. Med. Chem.* **1998**, *41*, 4607−4614.

(20) Kramer, M. S.; Winokur, A.; Kelsey, J.; Preskorn, S. H.; Rothschild, A. J.; Snavely, D.; Ghosh, K.; Ball, W. A.; Reines, S. A.; Munjack, D.; Apter, J. T.; Cunningham, L.; Kling, M.; Bari, M.; Getson, A.; Lee, Y. Demonstration of the efficacy and safety of a novel substance P (NK1) receptor antagonist in major depression. *Neuropsychopharmacology* **2004**, *29*, 385−392.

(21) McLean, S.; Ganong, A.; Seymour, P. A.; Bryce, D. K.; Crawford, R. T.; Morrone, J.; Reynolds, L. S.; Schmidt, A. W.; Zorn, S.; Watson, J.; Fossa, A.; DePasquale, M.; Rosen, T.; Nagahisa, A.; Tsuchiya, M.; Heym, J. Characterization of CP-122,721; a nonpeptide antagonist of the neurokinin NK1 receptor. *J. Pharmacol. Exp. Ther.* **1996**, *277*, 900−908.

(22) Ebner, K.; Sartori, S. B.; Singewald, N. Tachykinin receptors as therapeutic targets in stress-related disorders. *Curr. Pharm. Des.* **2009**, *15*, 1647−1674.

(23) Minthorn, E.; Mencken, T.; King, A. G.; Shu, A.; Rominger, D.; Gontarek, R. R.; Han, C.; Bambal, R.; Davis, C. B. Pharmacokinetics and brain penetration of casopitant, a potent and selective neurokinin-1 receptor antagonist, in the ferret. *Drug Metab. Dispos.* **2008**, *36*, 1846−1852.

(24) Ratti, E.; Bellew, K.; Bettica, P.; Bryson, H.; Zamuner, S.; Archer, G.; Squassante, L.; Bye, A.; Trist, D.; Krishnan, K. R.; Fernandes, S. Results from 2 randomized, double-blind, placebo-controlled studies of the novel NK1 receptor antagonist casopitant in patients with major depressive disorder. *J. Clin. Psychopharmacol.* **2011**, *31*, 727−733.

(25) Hoffmann, T.; Koblet, A.; Peters, J.-U.; Schnider, P.; Sleight, A.; Stadler, H. Dual NK1/NK3 Antagonists for Treating Schizophrenia. WO 2005/002577, 2005.

(26) Vauquelin, G.; Van Liefde, I.; Birzbier, B. B.; Vanderheyden, P. M. New insights in insurmountable antagonism. *Fundam. Clin. Pharmacol.* **2002**, *16*, 263−272.

(27) Malherbe, P.; Knoflach, F.; Hernandez, M. C.; Hoffmann, T.; Schnider, P.; Porter, R. H.; Wettstein, J. G.; Ballard, T. M.; Spooren, W.; Steward, L. Characterization of RO4583298 as a novel potent, dual antagonist with in vivo activity at tachykinin NK1 and NK3 receptors. *Br. J. Pharmacol.* **2011**, *162*, 929−946.

(28) Bromidge, S. M.; Catalani, M. P.; Heer, J. P.; Smethurst, C. A. P.; Tommasi, S. Novel Lactam Compounds. PCT Int. Appl. WO 2011054773, 2011.

(29) Catalani, M. P.; Alvaro, G.; Bernasconi, G.; Bettini, E.; Bromidge, S. M.; Heer, J.; Tedesco, G.; Tommasi, S. Identification of novel NK1/NK3 dual antagonists for the potential treatment of schizophrenia. *Bioorg. Med. Chem. Lett.* **2011**, *21*, 6899−6904.

(30) Lowe, J. A., 3rd; Drozda, S. E.; Snider, R. M.; Longo, K. P.; Zorn, S. H.; Morrone, J.; Jackson, E. R.; McLean, S.; Bryce, D. K.; Bordner, J.; et al. The discovery of (2*S*,3*S*)-*cis*-2-(diphenylmethyl)-*N*-[(2-methoxyphenyl)methyl]-1-azabicyclo[2.2.2]-octan-3-amine as a novel, nonpeptide substance P antagonisst. *J. Med. Chem.* **1992**, *35*, 2591−2600.

(31) Malherbe, P.; Bissantz, C.; Marcuz, A.; Kratzeisen, C.; Zenner, M. T.; Wettstein, J. G.; Ratni, H.; Riemer, C.; Spooren, W. Metalnetant and osanetant interact within overlapping but not identical binding pockets in the human tachykinin neurokinin 3 receptor transmembrane domains. *Mol. Pharmacol.* **2008**, *73*, 1736−1750.

(32) Palczewski, K.; Kumasaka, T.; Hori, T.; Behnke, C. A.; Motoshima, H.; Fox, B. A.; Le Trong, I.; Teller, D. C.; Okada, T.; Stenkamp, R. E.; Yamamoto, M.; Miyano, M. Crystal structure of rhodopsin: a G protein-coupled receptor. *Science* **2000**, *289*, 739−745.

(33) Cherezov, V.; Rosenbaum, D. M.; Hanson, M. A.; Rasmussen, S. G.; Thian, F. S.; Kobilka, T. S.; Choi, H. J.; Kuhn, P.; Weis, W. I.; Kobilka, B. K.; Stevens, R. C. High-resolution crystal structure of an engineered human beta2-adrenergic G protein-coupled receptor. *Science* **2007**, *318*, 1258−1265.

(34) Rosenbaum, D. M.; Cherezov, V.; Hanson, M. A.; Rasmussen, S. G.; Thian, F. S.; Kobilka, T. S.; Choi, H. J.; Yao, X. J.; Weis, W. I.; Stevens, R. C.; Kobilka, B. K. GPCR engineering yields high-resolution structural insights into beta2-adrenergic receptor function. *Science* **2007**, *318*, 1266−1273.

(35) Kenakin, T.; Jenkinson, S.; Watson, C. Determining the potency and molecular mechanism of action of insurmountable antagonists. *J. Pharmacol. Exp. Ther.* **2006**, *319*, 710−723.

(36) Malherbe, P.; Kratzeisen, C.; Marcuz, A.; Zenner, M. T.; Nettekoven, M. H.; Ratni, H.; Wettstein, J. G.; Bissantz, C. Identification of a critical residue in the transmembrane domain 2 of tachykinin neurokinin 3 receptor affecting the dissociation kinetics and antagonism mode of osanetant (SR 142801) and piperidine-based structures. *J. Med. Chem.* **2009**, *52*, 7103−7112.

(37) Jaakola, V. P.; Griffith, M. T.; Hanson, M. A.; Cherezov, V.; Chien, E. Y.; Lane, J. R.; Ijzerman, A. P.; Stevens, R. C. The 2.6 angstrom crystal structure of a human A2A adenosine receptor bound to an antagonist. *Science* **2008**, *322*, 1211−1217.

(38) Chien, E. Y.; Liu, W.; Zhao, Q.; Katritch, V.; Han, G. W.; Hanson, M. A.; Shi, L.; Newman, A. H.; Javitch, J. A.; Cherezov, V.; Stevens, R. C. Structure of the human dopamine D3 receptor in complex with a D2/D3 selective antagonist. *Science* **2010**, *330*, 1091−1095.

(39) Lindstrom, E.; von Mentzer, B.; Pahlman, I.; Ahlstedt, I.; Uvebrant, A.; Kristensson, E.; Martinsson, R.; Noven, A.; de Verdier, J.; Vauquelin, G. Neurokinin 1 receptor antagonists: correlation between in vitro receptor interaction and in vivo efficacy. *J. Pharmacol. Exp. Ther.* **2007**, *322*, 1286−1293.

(40) Topaloglu, A. K.; Reimann, F.; Guclu, M.; Yalin, A. S.; Kotan, L. D.; Porter, K. M.; Serin, A.; Mungan, N. O.; Cook, J. R.; Ozbek, M. N.; Imamoglu, S.; Akalin, N. S.; Yuksel, B.; O'Rahilly, S.; Semple, R. K. TAC3 and TACR3 mutations in familial hypogonadotropic hypogonadism reveal a key role for neurokinin B in the central control of reproduction. *Nat. Genet.* **2009**, *41*, 354−358.

(41) Silveira, L. G.; Tusset, C.; Latronico, A. C. Impact of mutations in kisspeptin and neurokinin B signaling pathways on human reproduction. *Brain Res.* **2010**, *1364*, 72−80.

(42) Cassel, J. A.; Daubert, J. D.; DeHaven, R. N. [(3)H]Alvimopan binding to the micro opioid receptor: comparative binding kinetics of opioid antagonists. *Eur. J. Pharmacol.* **2005**, *520*, 29−36.

(43) Copeland, R. A.; Pompliano, D. L.; Meek, T. D. Drug−target residence time and its implications for lead optimization. *Nat. Rev. Drug Discovery* **2006**, *5*, 730−739.

(44) Lacourciere, Y.; Asmar, R. A comparison of the efficacy and duration of action of candesartan cilexetil and losartan as assessed by clinic and ambulatory blood pressure after a missed dose, in truly hypertensive patients: a placebo-controlled, forced titration study. Candesartan/losartan study investigators. *Am. J. Hypertens.* **1999**, *12*, 1181−1187.

(45) Swinney, D. C. Biochemical mechanisms of drug action: what does it take for success? *Nat. Rev. Drug Discovery* **2004**, *3*, 801−808.

(46) Swinney, D. C. The role of binding kinetics in therapeutically useful drug action. *Curr. Opin. Drug Discovery Dev.* **2009**, *12*, 31−39.

(47) Ballesteros, J. A.; Weinstein, H. Integrated methods for construction three-dimensional models and computational probing of structure-function relations in G protein-coupled receptors. *Methods Neurosci.* **1995**, *25*, 366−428.

(48) Henikoff, S.; Henikoff, J. G. Amino acid substitution matrices from protein blocks. *Proc. Natl. Acad. Sci. U.S.A.* **1992**, *89*, 10915−10919.

(49) Wu, L. H.; Vartanian, M. A.; Oxender, D. L.; Chung, F. Z. Identification of methionine134 and alanine146 in the second transmembrane segment of the human tachykinin NK3 receptor as

reduces involved in species-selective binding to SR 48968. *Biochem. Biophys. Res. Commun.* **1994**, *198*, 961−966.
(50) Harrison, T.; Korsgaard, M. P.; Swain, C. J.; Cascieri, M. A.; Sadowski, S.; Seabrook, G. R. High affinity, selective neurokinin 2 and neurokinin 3 receptor antagonists from a common structural template. *Bioorg. Med. Chem. Lett.* **1998**, *8*, 1343−1348.